DTIC FILE COPY

②

AD-A231 822

REPORT DOCUMENTATION PAGE

Form Approved
OMB No. 0704-0188

1. AGENCY USE ONLY *(Leave blank)*

2. REPORT DATE
10/29/90

3. REPORT TYPE AND DATES COVERED
7/15/86 to 1/14/90 Final

TITLE AND SUBTITLE
Investigation of Schottky Barrier on GaAs and InP Using
a Multi-Disciplined Approach

5. FUNDING NUMBERS
Grant
AFOSR-86-0263,
mod/amend: C
Ref. No.: 169J027 (R)

AUTHOR(S)
Professor William E. Spicer

PERFORMING ORGANIZATION NAME(S) AND ADDRESS(ES)
Stanford Electronics Lab
McCullough Bldg.
Stanford University
Stanford, CA 94305

8. PERFORMING ORGANIZATION REPORT NUMBER
AFOSR-TR- 91 0024

SPONSORING/MONITORING AGENCY NAME(S) AND ADDRESS(ES)
AFOSR/PKD
Building 410
Bolling AFB, D.C. 20332-6448

Program Manager: Major Gernot Pomrenke (202) 767-4931

10. SPONSORING/MONITORING AGENCY REPORT NUMBER
2306/B1

11. SUPPLEMENTARY NOTES

12a. DISTRIBUTION/AVAILABILITY STATEMENT
Approved for public release;
distribution unlimited.

12b. DISTRIBUTION CODE

DTIC
ELECTE
FEB 15 1991
S B D

13. ABSTRACT *(Maximum 200 words)*

Major progress is reported in understanding and bringing under control metal/GaAs contacts. The key to this is the realization that defects at the interface can control the electrical propeties of such contacts. By properly controlling these defects it appears that the Schottky barrier height may be varied strongly to obtain the desired values for specific applications, i.e. large barriers for Schottky gates and small values for ohmic contacts. Evidence is presented that the key defects are As and Ga antisites. The Fermi level position at the interface, E_f, is the most important parameter in determining the electrical properties of the contact. Under normal conditions the As antisite levels dominate and the Fermi level is pinned near mid-gap. Producing excess As moves E_f toward the CBM whereas, excess Ga moves it toward the VBM. Experiments were first done with atomically clean interfaces and then the effects of a few layers of native oxides at the interface were investigated because native oxides are usually present in practical devices. It was found that the conclusions given above hold when oxide is present. Moreover, the oxide can enhance changes in interface morphology which can be critical for close spaced device geometry. They can also affect long term operation stability. This work gives a foundation for providing more optimum metal contacts and Schottky barriers on GaAs and for increasing productivity and reliability of monolithic as well as individual GaAs device systems.

14. SUBJECT TERMS

15. NUMBER OF PAGES

16. PRICE CODE

17. SECURITY CLASSIFICATION OF REPORT
UNCLASSIFIED

18. SECURITY CLASSIFICATION OF THIS PAGE
UNCLASSIFIED

19. SECURITY CLASSIFICATION OF ABSTRACT
UNCLASSIFIED

20. LIMITATION OF ABSTRACT
UL

AFOSR Report

I. Introduction

Work under this contract represents part of a major effort to bring the Schottky barriers on GaAs and other 3-5 semiconductors under control through fundamental understanding. The body of this report contains two major sections. The first is a chapter for a book, Defects in Metal/III-V Heterostructures by W. E. Spicer, in Defects in III-V Compound Semiconductors, Ed. Eicke R. Weber, Academic Press, Inc. This makes use of the major advances made under this contract and puts these in the general context of obtaining control of the GaAs/metal interfaces. The second part lists the important accomplishments under the contract and gives references to the article(s) published under the contract from which more details can be obtained. The purpose of this section is to give overall focus on the work actually done under this contract.

Prior and ongoing work at Stanford (under DARPA and ONR support) apply the newly developed techniques of photoemission spectroscopy (PES) and synchrotron radiation to studies of surface and interfaces. The present contract was the result of the realization that a closely coordinated program involving electric measurements on the same interfaces was necessary in order to make contact between the PES studies and the electrical properties of such interfaces. Thus, this program is distinguished from the original DARPA-ONR program in that it utilized electrical rather than electron spectroscopic measurements and was focused on the thick (1000Å) metal layers necessary for such measurements. The PES measurement requires much thinner films (order 1-10Å). The techniques developed in the PES work to provide atomically clean interfaces was also applied in this work. This removes a set of unknowns which has historically plagued studies of semiconductor/metal interfaces studies. In order to make contact with practical work (which is not usually done on clean surfaces) we prepared contaminated (i.e. are exposed) surfaces in a controlled way and studied the effects of such contamination of the interfaces. In this way we can make good contact with practical studies. (The list of publications contains a number of papers in which such results are reported.)

Since this overall study was motivated by a desire to understand GaAs (as well as InP and other 3-5) interfaces on an atomic level, we recognized that the electrical measurements give information best described as macroscopic not microscopic. In order to obtain more microscopic information on these interfaces we made use of electron-microscopic techniques,particularly TEM and EDAX, i.e. chemical analysis, techniques. This was done through collaboration with Dr. Z. Liliental-Weber at U. of California-Berkeley.

The procedure for the electron microscopic studies was one in which we made Schottky diodes with atomic control of the interface cleanliness. After diodes were formed under ultra high vacuum conditions, very careful electric measurements (I-V and C-V) were made on them. In some cases, the change of Schottky barrier height due to annealing was studied. The were then given to Dr. Liliental-Weber for electron microscopy studies. Results were studied by both groups and further experiments planned. Professor Eicke Weber at Berkeley, as expert in semiconductor defects was also a key collaborator.

Out of this work and the associated work (DARPA and ONR support) come several key concepts.

1. Defects play a key role in determining the electrical properties of metal/GaAs interfaces (DARPA-ONR support).

2. That the key defect for GaAs is the As antisite defect with the Ga antisite acting as a compensating center (Principally AFOSR support).

3. That the interface properties of GaAs can be controlled and changed in a constructive way not by making perfect interfaces; but by recognizing the nature of the imperfection and controlling this (AFOSR, DARPA, and ONR support).

4. Through control of (rather than elimination) of the defects at the interface, one has a possibility of controlling the electrical properties of such interfaces. (AFOSR, DARPA and ONR support).

The key parameter in determining the electrical properties of the GaAs interfaces is the position of the Fermi level at that interface. For this reason we will concentrate on this parameter in this report.

For ohmic contacts one would like the Fermi level to be near the appropriate band edge, i.e. the CBM for n- and VBM for p-doped materials. In the next section, we will present evidence that such a condition may be approached for n-GaAs. Our analysis indicates that this can be accomplished by properly manipulating the native defects and impurity doping near the interface. This is supported by results of studies by others as well as ourselves in which Fermi level motion as well as the GaAs/Pd/Ge ohmic contacts have been studied.

Similarly but less definitive evidence is presented showing that similar manipulation of native defects and impurities can produce ohmic contacts on p-GaAs.

Another key requirement for GaAs technology is optimum (usually large) Schottky barrier heights and stability of Schottky barrier heights and dimensions with processing and long term use (i.e. reliability). the experiments under this contract using thermal annealing, demonstrate how conventional Schottky barriers can be expected to change with time and also indicate how they can be stabilized so that such changes will not occur. Studies of thermal aging of GaAs microwave devices using Ti Schottky barriers by Varian Associates, Inc., will correlate with our studies of GaAs/Ti barrier heights with annealing.

For increased Schottky barrier heights on n- or p-GaAs, the same approaches as those for ohmic contacts should apply. For example, the procedures outlined to give ohmic contacts on n-GaAs would be modified to give large barrier heights on n-GaAs. Using knowledge of the factors causing changes in Schottky barrier height with aging, reliability of such Schottky barriers could be investigated and insured.

It is suggested that work under this contract has brought forward our understanding and ability to beneficially control metal/GaAs interfaces. In order to fully exploit these results more work is necessary.

Submitted for publication to Academic Press, Inc.
Book entitled "Defects in III-V Compound Semiconductors"
Ed. Eicke R. Weber

Defects in Metal/III-V Heterostructures

W. E. Spicer

I. Introduction

Since Bardeen's 1947 paper [1] we have become accustomed to the thinking of Fermi levels at metal/semiconductor interfaces as being highly pinned or fixed in energy. During the 1970's and early 1980's a literature developed which established that for GaAs it was difficult to move the interface Fermi level throughout the band gap (i.e. achieve inversion) at the native oxide interface. All of this has tended to fix in our mind the idea of a highly fixed and unmovable Fermi level at GaAs interfaces with either metals or insulators. Similar but less extreme effects were found for InP. However, in recent years there has been an increasing number of papers which report changes in the Fermi level position at GaAs and InP interfaces with accompanying changes in interface parameters of importance to devices and their application. These papers go back as far as ten years. Among the pioneers in this type of work were Grant and Waldrop at the Rockwell Science Center and Bachrach and Bauer at the Xerox Palo Alto Research Center. The purpose of this paper is to focus on work in which the Fermi level position at GaAs interfaces has been changed, and to provide a possible atomic level model as to what produces these changes.

It is not difficult to see the importance of Fermi level motion for device applications. If some degree of control can be obtained in the Fermi level at the interface, E_{fi}, this can be applied to ohmic contacts as well as Schottky barriers. For non-metallic interfaces, it could also lead to reduced surface recombination and even MIS devices. These are just some examples; there are many more. Ohmic contacts would be improved by moving E_{fi} to near the appropriate band edge. For Schottky barrier gates, the height of the barrier is important. If one can develop some degree of control of this height, devices and IC's can be made more optimally. For such applications, stability and predictability are also essential. This will be most easily obtained if we understand the interactions at the interface which cause Fermi level motion. Another area of importance is the semiconductor/insulator interface. At the lowest level of sophistication one may worry about surface recombination where such interfaces form boundaries of active areas of devices. Very large effects on devices performance have been demonstrated in specially designed devices[2]. A more sophisticated level would be the demonstration of a viable MIS device using GaAs. This has never been done. On InP, such devices have been demonstrated; however, time instabilities have kept them from being useful[3].

In the next section, several examples of Fermi level shifts due to various types of treatment of GaAs will be presented. Other examples could be given (see, for example, Ref. 4); however for brevity, only a few will be examined in detail here.

In many cases of E_{fi} change, a correlation with changes in Ga to As stoichiometry near the interface has been found. We also discuss this and interfacial metal/GaAs chemistry in Section II. In Section III we will discuss several models for Fermi level "position" at the interface and concentrate on a model which gives reasonable qualitative correlations with the changes in E_{fi} position and changes in stoichiometry. This model is based on a wide range of experimental data [4,5]. For example, certain pinning positions correspond almost exactly with the As_{Ga} antisite defect energy levels [6]. The model makes it possible to make a connection between shifts in the Fermi level and the GaAs/metal chemistry at the interface. Section IV touches briefly on recent work on GaAs insulator interfaces. This article will close with a section giving a summary, conclusions, and discussion.

II. Movement of the Fermi Level and Departures from GaAs Stoichiometry

A. Schottky Diodes

Newman and co-workers [7-9] have performed very careful experiments in which reproducible changes in barrier height were obtained by thermal annealing. Results are indicated in Figures 1 and 2. In order to reduce the number of variables, the diodes were formed on atomically clean GaAs surfaces formed by cleaving in ultra high vacuum (UHV). The atmosphere in which the annealing was done was found to be important for some metals. The usual procedure was to anneal the diodes in a N_2 atmosphere. (For Au/GaAs diodes different results were obtained when the annealing was done in vacuum.) It also proved important to separate out electrical leakage effects at the perimeter of the diode from change in the barrier height itself. This has been done for the data presented in Figures 1 and 2. Careful studies were made of Au[7,8], Al [7], Ti[10], Ag[7], and Cr[11]. The results are summarized in Table 1 [12]. Examining Figures 1 and 2, which are typical of those published by Newman and co-workers, it is important to realize that the shifts in the I-V curves (and thus in barrier height) are well beyond experimental uncertainty and that they are highly reproducible. A detailed discussion of reproducibility and experimental uncertainty is given in Reference 9.

From the Schottky barrier heights, φ_b, quoted in Figures 1 and 2, one can obtain E_{fi}. The zero for E_{fi} is taken at the VBM. Figure 3 gives the relevant energy level diagrams. The barrier height is the energy difference between the Fermi level at the interface, E_{fi}, and the conduction band minimum, (valence band maximum) for n-type (p-type). Thus for n-type material, as was used for the data of Figures 1 and 2 and Table 1, E_{fi} is obtained from the barrier height by the relation for

$$\text{(n-type)} \qquad E_{fi} = E_g - \varphi_b \qquad (1)$$

For p-type semiconductors, the relation is

$$\text{(p-type)} \qquad E_{fi} = \varphi_b \qquad (2)$$

Using these equations, the changes in φ_b given in Figures 1 and 2 can at once be translated into values of E_{fi}.

The key point here is that the Fermi level can be reproducibly changed by a processing step, thermal annealing, and that the details of movement depends on the metal used to form the Schottky barrier. Note that Al and Ti move E_{fi} toward the VBM, whereas Au moves it toward the CBM. No movement is seen for Ag and Cr.

What is the mechanism which determines this movement and how can the movement be controlled? In the next section, we will explore the relationship between interface chemistry, stoichiometry, and Fermi level motion. The purpose is to see if there are systematics which might help us begin to answer these questions.

B. Interfacial Chemistry and Departures from GaAs Stoichiometry

There is considerable literature concerning equilibrium reactions between GaAs and metals [13]. This data is extremely important but is still insufficient because it is thermodynamical data for the metal in equilibrium with the semiconductor. By definition, an interface is the boundary between two chemical systems which may or may not be in equilibrium. For example, living organisms (including human beings) are made up principally of carbon and exist in a world where they are surrounded by oxygen. Equalibrium thermodynamics tells us that the carbon should be oxidized to form CO_2. In layman's terms, this means that each human being should become a flaming torch until all of the carbon in our body is oxidized. Yet we are not unduly worried. The reason is that there are kinetic barriers to this oxidation which keep it from occurring. One can think of our skin as forming an interface with the oxidizing atmosphere surrounding us. There is a kinetic barrier between the O_2 molecules in the atmosphere and the carbon of our skin which prevents equilibrium being reached at room temperature. If the temperature is high enough, this barrier is overcome and we become, in reality, torches so that equilibrium can be achieved.

In a similar way, it is important to look not only at the thermodynamics, i.e. equilibrium chemistry, between metals and GaAs but also at the real interfaces and the effects of kinetic barriers on the chemistry and intermixing which takes place. Experimentally, it is well established that one can determine phase diagrams and the equilibrium chemistry by reacting the components to completion and analyzing the resulting compounds. It is much more complicated to examine interfaces in situations where kinetic barriers control the interface and equilibrium is not reached as is usually the case with semiconductor interfaces. In this article, we will concentrate on two types of experimental techniques to attack this problem: photoemission spectroscopy (PES) and electron microscopy (EM).

To apply photoemission spectroscopy, one evaporates a metal onto a clean GaAs surface in UHV and uses principally core level spectroscopy to follow the reactions taking place between the metal and semiconductor. PES and related electron spectroscopies are highly surface sensitive. Moreover, the depth probed can be changed by varying either the energy of the photoelectron (this can be done by varying the energy of the exciting photon) and/or by varying the angle of escape of the photoelectron with respect to the surface normal[14]. Figure 4 gives curves of electron escape depth versus electron energy for various solids. These data are for electrons emitted normally to the surface. The depth probed is reduced with angle by cos θ, where θ is the angle between the normal and the direction of escape of the electron.

Using PES from the atom core levels, one can obtain quantitative or semi-quantitative analysis of the chemical composition near the surface. Assuming an escape depth of 5Å (typical for 60 eV electrons in GaAs) one typically examines the first two or three atomic layers at the surface. If there were no reaction and if the deposited metal formed a uniform overlayer, one would exponentially decrease the electrons from the semiconductor which escape as more and more metal is deposited. A first-order equation for the probability of a photoelectron traversing uniform layer of deposited metal is:

$$P(x) = \exp(-\frac{x}{L}) \qquad (3)$$

where P(x) is the probability of transmission through a thickness, x, of the overlayer.

By examining the core level energies of the metal and semiconductor atoms one can determine what chemical reactions have taken place. By measuring the intensity of the various atoms as a function of the amount of metal deposited, one can determine the spatial distribution of the various atoms involved and thus determine whether or not there is diffusion, intermixing, surface segregation, etc. taking place. In this way insight can be obtained into the reactions taking place even in non-equilibrium, i.e. kinetically limited situations.

Figure 5 presents spectra of Ga and As 3d cores as a function of Ti coverage from the work of McCants [15]. Earlier studies for Ti can be found in the literature[16]. By deconvoluting the core spectra into surface shifted (clean GaAs) or reacted (due to Ti on surface) and bulk components, one can examine how the reaction goes with increasing amounts of Ti deposited on the GaAs. One can see by the large amount of reacted As and Ga produced that a strong reaction takes place even at room temperature. The amount of Ti deposited is given in terms of monolayers (ML) in Figure 5. A monolayer is taken to be 5.2×10^{14} atoms/cm^2 or 1.3 Å of Ti. The core levels of the substrate can only be detected with 5.3 ML (6.9Å) or less of Ti deposited. For the next thickness of 10.7 ML (13.9Å), no signal from the substrate is detected. This is consistent with an overcoating (Ti plus reacted Ga and As) which uniformly covers the GaAs (see Figure 4). Note that the amount of Ga seen within the probing depth of the experiment decreases strongly with the highest coverages; whereas, the As intensity does not. This indicates that the reacted Ga is being buried below the surface of the overlayer; whereas, the reacted As is not, i.e. the As is moving toward the free surface as the amount of Ti deposited is increased.

The deconvoluted As curves give evidence of two As-Ti compounds; however, only one broad peak is obtained for Ga. This Ga peak is consistent with Ga alloyed with Ti [17]. Note that the ratio of Ga and As peak strengths vary with coverage. This argues against the formation of stoichiometric compounds containing Ga, As, and Ti. Rather the lack of correlation for the higher Ti coverages indicates that reacted As and Ga are not distributed uniformly. Above all, one can draw the following conclusions:

- On a monolayer scale, a very strong reaction takes place at room temperature.
- The reaction products are complex and not uniformly distributed.
- The non-uniform distribution of the As and Ga gives evidence that equilibrium has not been reached within the reaction products.

These results are consistent with what might be expected from thermodynamics including heats of reaction or alloying when it is recognized that equilibrium has not been achieved.

Much data exists from photoemission studies done before high resolution and deconvolution schemes and other more sophisticated data analysis became available. To illustrate what may be obtained even from such studies, we will next examine spectra from several metals deposited on GaAs in Figure 6. These spectra are for the As 3d and Ga 3d core levels. Core spectra are given for various metal coverages. Changes in binding energy with metal deposition indicate As or Ga in a chemical site other than that for GaAs. In many cases better data is now available; however, these spectra (all taken with approximately the same resolution) allow a quick overview and illustrate the difference in interfacial chemistry without the complication of deconvolution [18-21]. In the raw binding energy PES data, there can be shifts due to chemistry and to band bending. Since we are only interested in the chemical shifts, the band bending shifts have been removed from the curves of Figure 6.

Ludeke et al. 22 have found that Ag does not react with GaAs. This is the only metal studies to date for which this the case. From the data of Figure 6, there is clear evidence of a reaction for each of these metals. For Au the Ga peak moves to a lower binding energy as one would expect [17] if the GaAu alloying expected from thermodynamics is taking place and the Ga is alloying with Au. Note that the Ga intensity decreases faster than for As. This indicates that the near surface region of the deposited Au is As rich. The binding energy shift of the As peak is small but toward high binding energy. This is consistent with the formation of elemental As and/or As weakly dissolved in Au and suggests that the reacted As is segregating to the surface.

From bulk thermodynamics [23], one would expect a saturated ternary solution (i.e. Au saturated, with about 1% Ga and As provided that one has a closed system (i.e. no As can escape). If As can escape then the Ga can alloy with Au up to about 10% or the AuGa, and $AuGa_2$ phases with higher Ga content can be produced. The PES data (open system but at room temperature so that the As vapor pressure is below 10^{-12} torr) suggests the presence of much more As than one would expect from thermodynamics. This is not surprising, since with the room temperature deposition it is unlikely that equilibrium would be reached.

Cu is similar to Au; however, Ni and Pd show strong shifts to higher binding energy for the reacted As. This is suggestive of formation of strongly bonded Pd/As and Ni/As phases as well as the Ga/Ni or Ga/Pd phases. Again, one would expect this from bulk thermodynamics [23]. However, the As density still has a tendency to be higher near the surface than for Ga. This suggests phase separation with surface segregation of As.

For Al, the reaction with GaAs has been well characterized by PES [24]. The reaction may be written schematically as:

$$GaAs + Al \dashrightarrow AlAs + Ga \qquad (4)$$

i.e. the Al replaces the Ga in the lattice forming AlGa and liberating Ga. If any As is liberated into the Al, it will quickly react to form AlAs. Operationally this means that the GaAs near the interface is transformed into an alloy, $Al_{1-x}Ga_xAs$, with either Al or Ga on the metal sites in the covalent lattice. For our future considerations here the key point is that free Ga but not As is produced at the interfaces.

Ti and Cr are included in the metals of Table 1. They fall into the class of Pd and Ni in Figure 6, i.e. the class where both Ga and As compounds or alloys are formed. Fortunately, Weaver's group has studied both Cr and Ti using PES. Importantly, they did *in-situ* thermal annealing and found that Ga but not As is expelled toward the free surface (UHV conditions) for Ti[15,25] whereas both As and Ga are held in the metal near the interface for Cr [25]. Thus that Ga may move out of the reactive phase leaving excess As for Ti but not Cr. For Cr, the annealing may not change the stoichiometry near the interface.

In Table 1 we have indicated whether excess As or Ga might be expected from the reaction of each metal with the GaAs. This is based on the PES studies discussed above. The reactions of Table 1 are those for the situation where one has a thick (order 1000Å) layer of metal on the GaAs. The condition of 1000Å metal layer plus the N_2 annealing gives a closed system. For Ag, Au, and Al the reactions are very clear cut and the conclusions straight forward. For Cr and Ti they are much more tentative and should be considered as reasonable possibilities until more data is available. If annealing were done in an open system so that the excess As can leave different results would be expected for Au. Such experiments were done and it was found that no change in the Fermi level occurred.

Next it is necessary to relate the changes in barrier height with annealing to reaction at the interface. The question is whether excess As or Ga at the interface is produced by the annealing. Such excess could serve as a source to modify the GaAs stoichiometry near the interface. Since we have a closed system, it will be the component which does not bind strongly with the metal which will be available to effect the GaAs stoichiometry. This is called the reaction product in Table I. For example, since As doesn't react strongly with Au it is the reaction product for Au/GaAs. Conversely the reaction product for Al/GaAs is Ga since Al, reacts so much more strongly with As.

III. A Model to Explain Fermi Level Movement

1) Introduction

There is no consensus as to the mechanism which gives rise to Fermi level "pinning" and Schottky barrier formation. In fact, there is growing thought that more than one mechanism may be important depending on the manner of Schottky barrier formation[5,26]. The proposed mechanisms can be placed in two classes. In the first or intrinsic class, the mechanism is operative for a perfect metal/semiconductor interface, i.e., it does not depend on defects or other departure from the ideal. A mechanism popularly called "metal-induced gap states" (MIGS) is the most widely accepted intrinsic mechanism[5,27,28]. In some cases it is reported that the original Schottky model [29] applies for specific GaAs surfaces [30]. This is also an intrinsic mechanism.

The second class of mechanisms [5, 27] depends on a departure from ideality at the interface, i.e. formation of interface levels due to a defective interface. The Unified Defect Model (UDM) [31] and its recent embodiment, the Advanced Unified Defect Model (AUDM) or Antisite Defect Model (ADM) [4,5,26], are based on native defects. The effective Work Function Model (EWF) [32] depends on the work function of elemental As at the interface determining the barrier height via a Schottky mechanism [29]. Ludeke has emphasized models which involve movement of the metal into the semiconductor forming doping levels and/or the changes in extrinsic and intrinsic levels at the interface[33].

These various mechanisms will now be considered in order to see if they can explain the observed changes in Fermi level pinning due to annealing. It is difficult to see how intrinsic mechanisms could explain this if the interface remains perfect. To be specific, the MIGS model as it has been presented to date does not appear able to explain this. In fact, Tersoff [34] has argued that the pinning due to MIGS is so strong that it is relatively independent of details of the interfacial region and depends mainly on the semiconductor alone. In response to these assertions of Tersoff, Zhang et al. [35] have shown theoretically that the MIGS are insufficient to screen out strong local interface potential effects on Schottky barrier heights. In particular, using Si they showed that by replacing the first Si layer at the interface with a layer of "donor" atoms (modeled on column V atoms), they could move the Fermi level by 0.28 eV toward the conduction band. In contrast, by removing the first layer of Si to create a potential barrier, they were able to shift the Fermi level by 0.27 toward the valence band maximum. Note that the total Fermi level motion by the two interface configurations is half the Si band gap. The work of

Zhang et al., to our knowledge, is the first which demonstrated that MIGS and extrinsic or defect mechanisms could work together to determine the barrier height. It is also important to recognize that it was the introduction of a non-ideal interface which caused the Fermi level movement. This reinforces one's intuition in concluding that extrinsic mechanisms must be introduced to explain Fermi level motion due to thermal annealing. In this paper we will attempt to explain E_{fi} movement in terms of defects. However, we do not reject the possibility that MIGS may also be playing a role in conjunction with the defects.

As mentioned above, a Schottky model has been suggested for certain specific GaAs surfaces. [29] However, to date this has not been found the case for practical GaAs contacts.

Let us examine extrinsic models of Schottky barrier formation. The systematics shown by the data of Table 1 are that the Fermi level moves toward the valence band when excess Ga is produced and toward the conduction band when excess As is produced. With this in mind let us explore the extrinsic mechanism discussed above.

First consider the EWF model [30]. The basis of the model is the suggestion that the barrier height is set by work function difference between elemental As and the metal. If changes are observed due to changes in the As excess, we only explain them in terms of changing the fraction of the surface covered by As. One would expect the reduction of As to make the metal work function more important. Al and Ti have low work functions compared to As [32]. Thus, for these metals one would, in the spirit of the EWF model, expect the barrier on n-type GaAs to be reduced on annealing (i.e. E_{fi} would move toward the CBM). This is the opposite of the experimental results. Since the work function of Au used in this model is equal to or larger than that of As [30], it does not appear possible to explain a decrease of barrier height for Au on n-GaAs due to annealing by this model. Thus, the EWF model is not attractive to explain the annealing results.

The approaches of Ludeke do not, by themselves, seem capable of explaining the data at this time. However, as they become more highly developed, they may become more applicable, either independently or in conjunction with other models.

2) Native defects and the Antisite Defect Model (ADM)

Spicer suggested in 1979 [30] that native defects determine the Fermi level at the interface. Allen and Dow[36], using a theoretical approach, first pointed out that the antisite defects (i.e. an As or Ga atom on the wrong lattice site) had properties which made it a strong candidate for being the dominant defects in the interfacial region. Independently, Weber et al. [37] found the energy levels due to the As_{Ga} (As on a Ga site) antisite defect and reported that they corresponded remarkably well with the pinning positions found experimentally by Spicer et al.[30] using PES and associated with native defects. Later Mönch [38,39] published a detailed analysis of GaAs pinning data and identified the importance of the Ga_{As} antisite. In 1987, Newman et al. [40] showed that annealing data for Al/GaAs (see Section IIA of this article) could be explained in terms of antisite defects. This led to the Advanced Unified Defect Model (ADM) [4,5,31].

The energy levels of the ADM are given in Figure 7. Near mid-gap are the donor levels of the As_{Ga} antisite. In Figure 8 is given a plot of the pinning positions found by Spicer et al. in 1979 [31] and the As_{Ga} antisite levels found by Weber et al. in 1982 [37]. As can be seen, there is strong agreement between these sets of levels[4]. It should be noted that these As_{Ga} antisites are now generally accepted as the levels responsible for the El-2 center in semi-insulating GaAs (see other articles in this volume). Just as for El-2, there must be a compensating deep acceptor in order for the mid-gap donor to affect n-type GaAs. We believe these levels to be the Ga_{As} antisites near the interface. For the Fermi level to lie near mid-gap, as is usually the case, the As_{Ga} antisites must outnumber the Ga_{As} antisites, i.e. the GaAs must be slightly As-rich at the interface. GaAs is usually grown under As-rich conditions [43], so that one expects the bulk to be As-rich and in fact there is notable evidence that this is the case. Evidence for excess As in LEC-grown GaAs is given by the ubiquitous presence of the El-2 center [44,45]. Evidence for excess As near the interfaces is given by the As inclusion on cleaved surfaces as reported by Bartels et al. [46]. It is also interesting to note that clouds of El-2 (and, therefore, of As_{Ga} point defects) form around dislocations in GaAs [47]. This suggests that the As_{Ga} antisites find a lower energy state in the distorted lattice near the dislocation and raises the question as to whether a similar lower energy state exists near free surfaces where the lattice is also distorted. For practical surfaces it should also be noted that As oxide is unstable in the presence of GaAs. In equilibrium, the As oxide will be transformed into Ga oxide with liberation of elemental As [48]. This can provide an additional source of As.

The difference in pinning positions of Al, In, Ga, and Cs found in 1979 (Fig. 8) for n- and p-type GaAs (Figure 8) was important because it allowed the two energy levels of As_{Ga} antisites to be identified. In 1979 those pinning positions were thought to be those under a metal since in each case they were found after enough metal to form a monolayer had been deposited. However, in 1983 Zur et al. [49] found that the pinning position must be the same for n- and p-type GaAs, and experimental work with thick (order 1000Å) metals on GaAs gave the same pinning positions on n- and p-type materials [40, 50]. Spicer et al. [51] have recently argued that the pinning observed in 1979 for Al, Ga, In, and Cs was that on non-metalized surfaces.

3) Fermi level movement due to excess As

One value of the ADM is that it gives a mechanism by which movement of the Fermi level at the interface, E_{fi}, can be explained. As can be seen from Fig. 7, the position of E_{fi} will be determined by the relative number of As_{Ga} double donors and Ga_{As} double acceptors. Based on this, let us examine how changing the ratio of As_{Ga} to Ga_{As} antisites densities can change the Fermi level position.

The probability that an available quantum state at energy (E) is filled with an electron is given by the Fermi-Dirac function,

$$P(E) = \frac{1}{\exp[(E - E_f) / kT + 1]}$$

Note that E_f is the energy at which the probability of a state being filled is one-half. At T = 0°K, P(E) reduces to a step function with all of the states above E_f empty and those below E_f filled (see for example, Ref. 52). Since the Fermi level will lay between the lowest lying empty state and the highest lying filled state, we can easily find its approximate position by counting states. For example, let us assume that the density of Ga_{As} antisites is just half of that of the As_{Ga}. The upper As_{Ga} donor will be empty and the lower full. As a result E_{fi} will lay halfway between them. If we increase the density of Ga_{As} acceptors, electrons will move from the bottom As_{Ga} donor level into these acceptor states, and the E_{fi} will move toward the VBM due to the reduced occupancy of the As_{Ga} states. At 0°K, E_{fi} would move into the lower level since it would become partially empty at higher temperatures, it would be above the lower level but closer to the lower than the upper level. If the density of Ga_{As} became larger than that of the As_{Ga} donors, the E_{fi} would move below the lower donor level at 0.5 eV. In contrast, if the As_{Ga} density increased, the Fermi will move toward the CBM. Thus, the ADM gives a possible connection between Fermi level motion and departures from stoichiometry of GaAs at the interface.

One thing that led to the ADM [4,5,31,42], was evidence in the literature of a correlation between Fermi level motion and departures from stoichiometry. For example, Bachrach et al. [42, 53], when studying MBE GaAs with PES, found a shift in energies of approximately 0.5 eV toward the VBM when the conditions in their MBE growth chamber were changed from As excess to Ga excess.

Svensson et al. [54] made measurements of E_{fi} on MBE grown under the usual As-rich conditions. Figure 9 shows the Fermi level positions they found on n- and p-type samples. The n- and p-type samples have different pinning positions similar to those found by Spicer et al. for Al, Ga, In, and Cs deposition [Fig. 8]. In addition, Svensson et al.

found that by increasing the amount of excess As at the surface of the GaAs, the E_{fi} could be moved toward the CBM for both n- and p-type GaAs as the ADM predicts.

Workers at the Optoelectronics Joint Research Laboratory in Japan studied Schottky barriers of LaB_6 on GaAs [55] because lack of strong chemical reactions of LaB_6 with GaAs makes it of interest for self-aligned gate technology. Studies were made of LaB_6 on both MBE and chemically prepared (100) surfaces. In the case of MBE, *in-situ* measurements of the Fermi level position at the surface were performed on thin layers (up to a few monolayers) of LaB_6 deposited and thermally annealed. Thick (1800Å) films were deposited on both the MBE and chemically prepared surfaces, and electrical measurements were performed to determine the Schottky barrier height as a function of annealing. For both the MBE thin film studies and the thick studies, the effects of annealing were related to As loss.

The results of these studies are shown in Figure 10. Here the data on E_{fi} is plotted as CBM-E_{fi}, i.e. the reference point is taken as the CBM, not the VBM as in the rest of this article. In the upper panel, one has E_{fi} for the MBE samples. (CBM and VBM are the conduction band minimum and valence band maximum, respectively.) As grown, the surface is As-rich, and the E_{fi} lies near the upper As_{Ga} antisite level of Figure 7. When As is removed, either by annealing and/or by deposition of the metal, E_{fi} moves toward the VBM (i.e. CBM-E_{fi} gets larger). For thick LaB_6 layers (1800Å), the same effect was observed on annealing for MBE (As-rich) or chemically etched samples, with the difference that the MBE samples took more annealing to produce the Fermi level motion than did the chemically etched sample. This is reasonable since greater As excess would be expected in the starting MBE than the chemically etched samples. The systematics of the Fermi level moving toward the CBM with excess As and toward the VBM as this excess is reduced was once again found.

Very important experiments have been performed by Waldrop and Grant [56,57] in which they were able to move E_{fi} from below mid-gap to within 0.2 eV of the CBM. The key was the evaporation of 6 to 14 Å of Ge in a As_4 atmosphere onto a clean GaAs(100) surface held at elevated temperature (200°C to 325°C). If the Ge was deposited without the As_4 over pressure, the Fermi level movement did not take place. The rate of arrival of Ge and As_4 at the GaAs surface seemed to be comparable. A LEED pattern was obtained after the Ge(As) was deposited showing that it was crystalline. *In-situ* studies were made of the band bending using PES. Samples were also made with thick Au or Ni overlayers for electrical measurements. PES results were compared to those obtained from I-V measurements. Figure 11 shows the E_{fi} position (E^i_f in the terminology of Grant and Waldrop) obtained by PES for various layers on GaAs. Without excess As (i.e. an As over pressure) E_{fi} is in a typical position for a GaAs interface, (i.e. near mid gap); however, with As the Fermi level position typically rose to between 1.0 and 1.2 eV above the VBM[56]. Once again we see a correlation with movement of E_{fi} toward the CBM and excess As. Here E_{fi} gets much closer to the CBM than in the cases we have discussed previously. A possible reason for this will be given presently.

Figure 12 reproduces the I-V curves obtained by Waldrop and Grant [56]. The curves for: Au - NiAs - 9 Å Ge (As) and Au - 100 Å Te - 7 Å GeAs are believed to correspond to the PES films of Ge (As). The Te or NiAs layers were added to keep the Au or Ni from reacting with the Ge. For these films the Schottky barrier height on n-GaAs was approximately 0.25 to 0.4 eV, i.e. E_{fi} was 1.0 to 1.15 eV above the VBM in agreement with the PES studies. However, without the Ge(As) layer a much different E_{fi} position was found. Note the Au-GaAs case shown in Figure 12 where Au was deposited directly on a clean GaAs surface, the barrier height was 0.89 eV corresponding to an E_{fi} 0.51 eV above the VBM. Thus, the Ge(As) layer gives an E_{fi} upward movement of over 0.5 eV.

An earlier example of E_{fi} movement due to excess As and Ge is given by the work of Chiaradia, et al.[58]. Using MBE techniques, the Fermi position on a GaAs(100) surface was first studied as a function of As or Ga excess in the starting GaAs(100) surface. The results are shown in Figure 13. For a C(4x4) reconstructed surface (corresponding to at least a monolayer of excess As) E_{fi}, is approximately 0.7 eV above the VBM; whereas, for a C(4x6) reconstruction (at least 3/4 of a monolayer of Ga) E_{fi} is located at about 0.45 eV above the VBM. Note that these positions are close to the upper (0.75 eV) and lower (0.5 eV) levels of the defect model and the As_{Ga} antisite defect with excess As putting E_{fi} near the upper level and excess Ga putting E_{fi} near the lower level.

Also shown in Figure 13 is E_{fi} for a C(8x2) reconstruction which has excess As but less than the C(4x4) surface. As can be seen, the Fermi level on this free surface is near but lower than that on the C(4x4) surface. The difference is in agreement with the prediction of the ADM. There is also data in Figure 13 for a n-type GaAs(110) cleaved surface. Here the original position of the Fermi level is at the CBM. This is because of the perfection of this surface which contains few defects and the fact that it reconstructs so that the dangling band surface states are swept out of the band gap [59] thus leaving insufficient surface states to move E_{fi} from the bulk position.

In Figure 13, the effect of adding Ge to the various GaAs surfaces is also shown. For all GaAs(100) surfaces, the movement is toward the CBM; however, the more As excess present in the starting surface, the greater the movement. These results are summed up in Figure 14 which gives a band diagram for the GaAs/Ge interface including the E_{fi} positions for the three different starting GaAs(100) faces.

In Fig. 15 we show the Fermi level development for Ge deposition is an As_4 ambient. The data in Figure 15 suggested to Chiaradia et al. that the Fermi level movement with Ge deposition was associated with As moving into and doping the Ge. The work of Mönch et al. [60] indicates that such As diffusion (and to a much lesser extent Ga) takes place even without the presence of excess As at the original surface.

The material above gives additional strong empirical correlation between excess As and movement of the Fermi level. We suggest that this might be explained in detail by the ADM; however, the reader should remember that these empirical correlations are experimental results which are independent of any model. Furthermore, even though I show that these results can qualitatively be explained by the ADM, I do not show this explanation to be unique.

Figures 16a and b indicate our suggestions for the interpretation of the data of Waldrop and Grant [56,57] and Chiaradia et al. [58]. Because of the lattice match between Ge and GaAs, the defect density near the interface may be reduced. However, as long as Ga_{As} antisites or other low lying acceptors are present, the Fermi level can not move much above the upper As_{Ga} antisite level. Even, if the population of As_{Ga} antisites is much larger than that of Ga_{As} antisite, there will be a density of holes in the upper (0.75 eV) As_{Ga} antisite level equal to twice the density of Ga_{As} antisites (assuming that these antisites are double acceptors). Because of this, it will be difficult for the Fermi level to move much above the upper As_{Ga} level (see Equation 5) unless there is a source of electrons to fill these states (as shown in Figure 16a). For the free surface, a clear source of such electrons are the donors which are emptied to produce band bending and the depletion, n_d. In addition, if a n-doped Ge layer is present as in the experiments just discussed, then it also may contribute electrons, n_d, to fill the empty interfacial states. The density of empty As_{Ga} states, n_e, will be given by:

$$n_e = 2N(Ga_{As}) - n_d - n_l \qquad (6)$$

where N(GaAs) is the density of Ga_{As} antisites and n_l is the density of electrons donated from the doped Ge overlayer.

$$n_d = \sqrt{2\varepsilon_{ss}\, qN_d V_{bb}} \qquad (7)$$

in MKS units. Here ε_{ss} is the permittivity of the semiconductor, ($\varepsilon_{ss} = Ke_o$, where K is the dielectric constant and e_o is the permittivity of free space), N_d is the density of uncompensated donors (for n-GaAs), q is the magnitude of the electron charge, and V_b is the magnitude of the voltage drop across the depletion region, i.e. the amount of band bending.

If n_e in Equation 6 is less than zero, it simply means that all of available defect states have been filled with electrons, and E_{fi} will move above the highest lying defect level toward the CBM. In order to find the exact position of E_{fi}, one would have to solve properly Poisson's equation with the correct parameters. This situation is shown schematically in Figure 16b.

Studies similar to those of Ge on GaAs have been performed by Mahowald et al.[61, 64] on InP. There is an important difference, however. No P was added to the Ge for n-type doping. Rather, the PES studies [55,62,63] suggested that the Ge slightly attacked the InP producing primarily P in the InP and In segregated to the surface. The P in the Ge is believed to leave it highly n-doped. Experimental data for the E_{fi} position as a function of Ge coverage is presented in Figure 17. The starting InP surface was (110) cleaved. As can be seen for both n- and p- InP, E_{fi} initially moves to a position about 0.4 eV below the CBM. Then, for higher coverages, E_{fi} moves toward the CBM.

Mahowald et al.[61-63] modeled these results in terms of Poisson's equation, charge neutrality, and certain assumptions. We will now outline the principle assumptions. For the first 0.5Å of Ge deposition, the defect concentration in the InP is assumed to increase at a linear rate of 3×10^{13} defects/Å of Ge. For Ge thickness greater than 0.5Å, it is assumed that no new defects are formed near the InP/Ge interface. For Ge coverages greater than this amount, it is assumed that P donors are added to the Ge at a rate of 3×10^{13} donors $\text{Å}^{-1}\text{cm}^{-2}$, which is equivalent to 21.5×10^{20} donors/cm^3. The defects were taken to be a donor at 1.1 eV and an acceptor at 0.9 eV above the valence band maximum. In the AUDM this will be equivalent to column V antisites outnumbering the column III antisites by two to one so that the highest antisite donor state would be completely empty and the lowest completely filled.

The shaded line in Figure 17 indicates the calculated Fermi level position as a function of Ge coverage based on these assumptions. As can be seen, the calculated E_{fi} positions closely follow the experimental data. This at least demonstrates that such data can be modeled in terms of a defect model such as the ADM. Preliminary work indicates that this model also works for GaAs.

4) Ohmic Contacts on n-GaAs

The reader has probably realized, as did the authors quoted, the importance of this work to development of ohmic contacts on n-GaAs. We will now address this question. Ohmic contacts on both n- and p-GaAs have always presented a problem. In recent years this has become more serious for some GaAs IC's because of reduced dimensions. Through most of the history of GaAs, the approach to ohmic contacts was almost solely empirical. It is only in recent years that a more scientific approach has been taken for ohmic contacts. The work of Waldrop and Grant[56,57] referred to earlier is a good example of this. The work of S. S. Lau and his co-workers[64] on the Pd/Ge/GaAs contact is another example of this which has been carried forward to establish a new ohmic contact technology on n-GaAs. The contact often being replaced by Pd/Ge/GaAs is the Ni/Au/Ge/GaAs contact. One difficulty with that contact is that the metal/GaAs interface is not atomically smooth but contains irregular protrusions which can extend 100's of Angstroms into the GaAs. These protrusions not only can penetrate and thus destroy thin device structures but they also make it very difficult to use electron microscopy and related tools to study the interface. One of the advantages of the Pd/Ge/GaAs contact is that it forms smooth interfaces without the protrusions. This makes it possible to analyze the interface in detail (see Fig. 18). It has been established that the GaAs within about 40Å of the interface is regrown and is highly doped with Ge[64,65] after the contact has been thermally processed. The top panel in Fig. 18 shows the structure of this contact. There are arguments against the Ge layer being highly doped with As[64]; however, we believe that it is best to keep this possibility open for the purpose of this discussion.

The bottom panel in Fig. 18 gives a band diagram for this contact. The Schottky barrier between the GaAs and the Ge is shown to be 0.3 eV, in agreement with the data of Lau et al. and co-workers for the resistivity of the contact as a function of temperature (see the middle panel of Fig. 18 for schematic drawing of this). This means that the Fermi level has moved from its typical position near mid gap to within 0.3 eV of the CBM. Thus, the ohmic behavior is due to both the heavy doping of the GaAs giving a tunnel junction (see the middle panel of Fig. 18) and to a reduced barrier height due to the Fermi level movement. Previously, it has usually been assumed that the Fermi level was well pinned near mid-gap and that the tunneling had to be thought a much larger barrier than that reported for Pd/Ge/GaAs. The results and arguments given here indicate that this is not the case and that E_{fi} can be moved if the optimum conditions are achieved.

We would explain this contact in terms of the mid gap interface states being completely filled by electrons from the strongly doped GaAs in the depletion region and As doped Ge in accordance with Equation 6. On an atomic level, we would use the ADM to explain this. Since Ge and GaAs have an almost perfect lattice match and the heavily doped GaAs next to the Ge has been regrown in the process of forming the contact, we suggest that the density of interfacial defects has been reduced, i.e. n_e in Equation 6 has been reduced, by lowering the density of antisites. Further we assume that enough electrons go into these interface states from the depletion region, n_d, and the doped Ge, region n_I, to completely fill the mid-gap interface states. As a result E_{fi} moves up to near the Ge CBM which is about 0.2 eV from the GaAs CBM. Note that in Equation 6, it is the density of Ga_{As} antisites, N(GaAs), not the total density of antisite defects which determine n_e. One would expect a reduction in this density if the GaAs regrowth took place under strongly As rich conditions. This may be case here for two reasons. First, since the bulk GaAs is As rich and, as discussed earlier, excess As seems to segregate to interfaces, this will also produce a source of excess As. A second source may be produced because the Pd (which is originally in contact with the GaAs thermal anneal) appears to react with GaAs releasing As.

The reader's attention is also directed to the relationship of this contact to the work of Waldrop and Grant and the Xerox group on the motion of the Fermi level due to As doped Ge on GaAs. This gives direct evidence that the Fermi level can be moved in a closely related system. Note also that, in this previous work, one depended solely on the doped Ge to provide the electrons to generate the Fermi level movement. However, with the ohmic contact, one has not only this source of electrons but the electrons from the highly doped depletion region which is formed during the thermal anneal (see Equation 7).

It is reassuring that so much concerning the Pd/Ge/GaAs contact is consistent with the ADM; however, one must be always remembered that we have established consistency and not uniqueness. Other studies are now underway to test the application of the model to this ohmic contact more quantitatively and to test materials parameters critical to the explanations given above.

The attractiveness of the ADM lies not in its ability to explain one contact or observation but to explain a large range of behavior not only at metal-GaAs interfaces but also at insulator GaAs interfaces. We will examine one such situation in a later section.

5) Fermi Level Movement Due to Excess Ga

The last set of experimental data we would like to discuss in this section is that relating to Ga on GaAs. If Ga deposition could lead to an increase in Ga_{As} antisite acceptor density, it would move E_{fi} toward the VBM. Strong movement of E_{fi} toward the VBM due to evaporation of the thin Ga-layers for PES studies has not been observed. However, the studies of Cao show a trend in that direction [66]. Bolmont et al.[67] has reported that new states below the E_f are created by Ga deposition. This is consistent with Ga_{As} antisite formation. However, the situation is quite different for thick layers of Ga deposited in various ways on GaAs. Table 2 summarizes results from five electrical studies of barrier heights for thick Ga on GaAs. Four of these indicate E_f positions surprisingly close to the VBM. This data is striking in that the barrier heights on n-GaAs are perhaps the highest (about 1.1 eV) reported for any metal on GaAs. In the past, changes in barrier with metals have been found to correlate with electronegativity, i.e. E_{fi} positions well away from the

VBM for electropositive materials. On n-GaAs lower electronic negativity is found to correlate with low electronegativity. Metals such as Al and In are very close to Ga in electronegativity and have barrier heights of about 0.8 eV on n-GaAs. This is in contrast to the values near 1.1 eV for the thick Ga/GaAs samples. The highest electronegativity metals such as Au and Pd have lower barrier heights (0.9 - 1.0 eV). However, a word of warning is necessary. Problems of leakage plagued I-V measurements for Ga/GaAs Schottky barrier, and some of the results in Table 2 are from C-V measurements which are not as reliable. The I-V curves of Reinke and Meming are excellent; however, there evidence for excess Ga is not direct.

MBE techniques may be the best suited for such studies. In fact, the studies of Svensson et al.[68] are perhaps the most satisfying of those included in Table 2 because their methods of forming the Ga/GaAs seemed most clean cut. However, in order to understand Ga/GaAs more completely, it is necessary that well controlled experiments be done in which both the electrical properties of the contacts and the arrangement of atoms near the interface are sufficiently well specified.

The data presented in Table 2 and discussed above can be explained in terms of the ADM (see Figure 7). If Ga is deposited in such a way that the population of Ga_{As} antisites is sufficiently enhanced, then it is reasonable that the Fermi level would move into the vicinity of the Ga_{As} antisite levels, i.e. near the VBM as observed.

In this section we have outlined the ADM and shown some of the data which seems to be consistent with it. In the next section we will examine evidence for departures from stoichiometry at the interface and see how this relates to "predictions" of the ADM. We put predictions in parenthesis because some of the data in the next section played a role in development of the ADM.

6) Measurements of Departures from Stoichiometry at the Interface and Their Relation to the ADM

The ADM predicts certain departures from stoichiometry at the GaAs interface. For E_{fi} to lie above approximately 0.5 eV, one needs a greater density of As_{Ga} than Ga_{As} antisites and, thus, an As excess. In order for the As_{Ga} population to dominate it is likely that a much larger As excess exists at the interface than is represented just by the excess As in antisites. This is a situation similar to the enhanced As and El-2 (i.e. As antisite) densities at dislocations [69]. Earlier in this article, changes in Schottky barrier height and, thus, E_{fi} on annealing have been correlated with changes in stoichiometry expected in terms of interfacial chemistry. (See, for example, Table 1). It is important to test experimentally whether such correlations actually exist. Liliental-Weber and co-workers have used Energy Dispersive X-ray (EDX) analysis to examine the interfacial stoichiometry [11,70,71] for several metals (see Table 3). Pallix et al. [72] have used a new technique, Surface Analysis with Laser Ionization (SALI), to study the stoichiometry of GaAs/Au interfaces before and after annealing.

Let us first examine the SALI results. There is a great difficulty in examining interfaces for excess As if that As is not firmly tied into the lattice. The reason for this is the low vapor pressure of As combined with its high energy of ionization. As a result, excess As which may be loosely bound to the GaAs is easily desorbed without ionization. Unfortunately, the tools of surface analysis which might be used to detect the excess As impart energy into the surface region which can cause such desorption. The key to the SALI techniques is that it ionized any atoms which leave the surface by means of a laser. Thus, it is peculiarly sensitive to loosely bound As. The SALI results for the GaAs/Au system are given in Figure 19 [72]. As can be seen, a strong As build-up at the interface after the annealing is found, in qualitative agreement with expectations from the ADM.

The EDX method used by Liliental-Weber is based on using a very fine high current density electron beam to excite the core levels of atoms so that they emit characteristic X-rays. It has a lateral resolution of about 100Å. One would expect such a beam to cause desorption of loosely bound As. In essence this was what was found.

Excess As was found but this decreased as the electron beam was left on one spot. The key parameter is the ratio of As to Ga X-ray luminescence intensity. When the beam was placed at the GaAs/Au interface, an increase in the As/Ga ratio was seen over that for the GaAs away from the interface. The excess As signal decayed with time until it returned to the value seen from the GaAs away from the interface. As Table 3 shows, excess As was always found at the interface after metal deposition (in agreement with the ADM). After annealing, the increase or decrease of As excess was found to correlate with Fermi level movement in a way consistent with the ADM (see Table 3). There is an unexplained discrepancy between the SALI GaAs/Au and the EDX results. EDX showed an As excess after Au deposition but before annealing. However, as can be seen from Figure 19, there is no clear evidence of this from the SALI results. This may be due to detailed differences in the two techniques. However, it emphasizes the fact that much more work should be done in studying departures from stoichiometry at GaAs interfaces in order to be certain of the results.

In this section we have shown an experimental correlation between departures from stoichiometry at GaAs/metal interfaces and Fermi level movement. This strengthens the suggestion that Fermi level position and thus the electrical properties at interfaces may be controlled by departures from stoichiometry. However, it must be recognized that the presence of excess As or Ga at the interfaces alone is insufficient to explain Fermi level movement in terms of antisite defects. One must assume that the excess leads to an increase of As_{Ga} or Ga_{As} in the interface region of the GaAs crystal. This means that As or Ga must be incorporated in the GaAs as antisite defects. The kinetics of this is an important question which has not been addressed in this paper but which must be addressed in the future. It is easier to understand how this incorporation can take place in the annealing experiments rather than experiments in which Ga is simply deposited on a GaAs surface held at room temperature. This may explain some of the difficulties in studying such deposition of Ga on GaAs. MBE is very important since it provides a way of more directly incorporating excess As or Ga into the lattice. The limited number of results with this method provide one of the best sets of evidence of Fermi level motion associated with departures from stoichiometry. Much more work is needed on the kinetics of antisite inclusion in the interface region.

IV. GaAs/Insulator Interfaces

Two types of interfaces are critical in order to bring GaAs device and integrated circuit under control. The first, GaAs/metal interfaces, has been treated in the previous sections. In this section we will touch on the second type of interface - the GaAs/insulator interface. In this category we include all GaAs surfaces not covered by metals whether the insulator is consciously deposited or is a result of GaAs oxidation. In the 1970's a strong effort was made to develop a MOS technology for GaAs similar to that of Si. This failed. It became clear that the chemistry between GaAs and its oxides did not lead to a chemically stable, defect-free interface[74]. Due to this, the hope of a GaAs MOS technology was abandoned and work concentrated on a field effect transistor (FET) technology in which a Schottky barrier or a p-n junction provided the control element for the device. However, even with these technologies, there are GaAs surfaces not covered by the control structures. These surfaces plague GaAs devices and IC's for several reasons. For example, they usually have a very high surface recombination which can degrade device operations. In addition, it is hard to control this potential and this can lead to "side gating" and other unpleasant occurrences which disrupt device and/or IC operation.

In recent years three new and promising approaches have come forward to provide better control at such surfaces. These may also lead to MIS technologies. In the first of these a heterojunction is made with a higher band gap semiconductor which has a sufficiently good lattice match so that a good heterojunction is formed. $Al_xGa_{1-x}As$/GaAs and GaAs/ZnSe are examples[75]. Here, it has been shown that interface (surface) state density can be kept relatively low. The main difficulty with such an approach is the difficulty in forming a sufficiently ideal heterojunction and the limitation due to the relatively low band gap of the "capping" semiconductor. A second approach is just in its early stages [76]. This starts with the deposition of a Si layer on the GaAs. Then an insulator (for example, SiO_2 or Si_3N_4) is grown. Again this shows promise but it is in the early stages of development and testing. In the third approach, striking success in reducing surface recombination has been achieved[77] by treating GaAs surfaces with the sulfur compounds $Na_2S \bullet H_2O$ or $(NH_4)_2S$. We will discuss this in more detail since a number of measurements have been made of the Fermi level position and changes therein due to such treatments.

Use of sulfur passivation approach has recently been reviewed by Spindt and Spicer [76]. As emphasized in that paper, the principal criteria for passivation by this approach is the reduction of surface recombination by more than two orders of magnitude. It was first suggested that the treatment removed interface states so that the Fermi level at the interface moved from mid gap to the bulk Fermi level position[75] near the CBM. However, measurements of Fermi level position using a number of different techniques showed that this was not the case[79-83]. Rather the treatment moves the Fermi level closer to the VBM on n-GaAs. Spindt and Spicer[84] have suggested a model to explain this behavior. This model is based on the ADM and suggests that the sulfur treatment removes excess As and thus As_{Ga} antisites from the surface. As we established in a previous section, if the As_{Ga} density is reduced relative to the Ga_{As} antisite density, the Fermi level must move toward the VBM in accord with the experimental observations.

Results from Besser and Helms[79,85] for the Fermi level position as a function of surface treatment is shown in Figure 19. As can been seen the Fermi level moves from the vicinity of the upper (0.75 eV) level of the As_{Ga} antisite level to the vicinity of the lower (0.5 eV) As_{Ga} antisite level due to the sulfur treatment. As Spindt and Spicer noted, this results not only in the change in band bending but also in the As_{Ga} antisites becoming positively charged. With the interface Fermi level near 0.5 eV, one has the bands bending upward with a barrier of about 0.9 eV that electrons must overcome to reach the surface. Holes will be swept into the interface by the band bending, but they will be inhibited from recombining with electrons on the mid-gap As_{Ga} states since this double donor is compensated so that it has a single positive charge and will repel them. Thus, surface recombination will be reduced.

Figure 21 shows the change in band bending found by a number of workers using diverse experimental approaches [78] and indicates how this is explained in terms of ADM. The key to application of the ADM is the assumption (supported by some experimental findings [78]) that the As_{Ga} to Ga_{As} ratio is reduced by the sulfur treatment's preferential removal of As from the GaAs surface region. As explained in Section III, this will cause the Fermi level to move toward the VBM because of depletion of electrons from the As_{Ga} donors by the Ga_{As} acceptors. The fact that E_{fi} moves approximately to the lower As_{Ga} level at 0.5 eV indicates that the As_{Ga} is a little more than half compensated. This results in the As_{Ga} defect having a positive charge which repels holes and thus inhibits the surface recombination as discussed above.

Figure 22 shows surface DLTS results from Liu et al[80] before and after the sulfur treatment. Note that before treatment there is large density of states centered near 0.85 eV. This we associate with the upper As_{Ga} level. After the treatment, the dominant levels are at 0.3 eV above the VBM. Thus we associate with the Ga_{As} levels.

Much more must be done before the "free" and/or insulator/GaAs surfaces and interfaces can be brought under sufficient control. However, the sulfur example illustrates the importance of Fermi level movement in this. We would argue that one must measure and understand the physical and chemistry driving Fermi level motion at the interface and the consequences of such movement before control can be obtained of these interfaces. We also note that interface properties such as recombination can be improved without obtaining ideal passivation which includes a flat band condition.

V. Conclusions and Discussion

This article gives strong evidence that the Fermi level at GaAs metal interfaces can be varied by a good fraction of the band gap. For instance, Waldrop and Grant [56,57] were able to move the Fermi level with about 0.3 eV of the CBM and Svensson et al. [68] were able to move it to within about 0.3 eV of the VBM. Many other examples have been given here of Fermi movement associated with special deposition conditions, thermal annealing or other treatment. A surprisingly consistent thread runs through most of the work described. This is a correlation in the change of GaAs stoichiometry at the interface with the direction of motion of the Fermi level. When the Fermi level moves toward the CBM an increase of As excess is found. Fermi level movement toward the VBM is associated with an increase in the relative amount of Ga at the interface. Using this, the interfacial chemistry between the metal and GaAs can be used to predict Fermi level movement due to thermal annealing.

A model for the electrical properties of the interface, the Antisite Defect Model (ADM)[4], has been introduced to explain the changes in Fermi level. This model is based on the conclusions that As_{Ga} antisites and Ga_{As} antisites provide the energy levels which are dominant in determining the Fermi level position (Figure 7). The As_{Ga} is a double donor with levels at 0.75 and 0.5 eV above the VBM. The Ga_{As} antisite is a double acceptor with levels near 0.3 eV. By assuming that the relative numbers of these two defects changed in accordance with changes of stoichiometry near the interface a large number of experimental results can be explained.

Much more work must be done to fully test the correlations made here. The ADM must also be tested further. However, the agreements with experiments are sufficiently strong that one might use the correlations and/or the ADM to attempt to solve practical problems. Ohmic contacts are one such problem for GaAs device and IC development and applications. It is the ohmic contact which limits many devices. Most work developing ohmic contacts to date has been strongly empirical. Perhaps the ideas presented might be applied in an attempt to develop better ohmic contacts. Usually ohmic contacts on GaAs are thought to be tunneling, i.e., even though a large Schottky barrier is present, the doping of the GaAs near the interface is so high that a narrow depletion layer is formed through which the carriers can tunnel through. This demands very high doping due to contact formation. However, if the Fermi level can be moved in a favorable direction, the ease of tunneling will increase exponentially. Thus, a combination of Fermi level movement and doping may be essentially for developing a better ohmic contact technology. This approach does give the possibility for new ways to think about and develop ohmic contacts. As indicated in Section III-4, this approach seems to explain the Pd/Gd/GaAs ohmic contact on n-GaAs.

Most of this article has concentrated on metal/GaAs interfaces. Another set of systems in which better control is needed are the GaAs/insulator interfaces. These were briefly discussed and it was shown that data on sulfur treated interfaces could also be qualitatively explained by antisites and the AUDM. There is need of much more work on such interfaces to bring them under control and stop them from limiting the usefulness of GaAs. Above all there is a need to move from strongly empirical approaches to approaches in which sufficient characterization is done to be able to understand and model these interfaces.

Acknowledgement:

Useful discussions with Nate Newman, Eicke Weber, Zuzanna Liliental-Weber, Ken Miyano, Renyu Cao, Tom Kendelewicz, Chris Spindt, Paul Meissner, and S. S. Lau are gratefully acknowledge. This work was partially support by DARPA and ONR through Contract # N00014-89-J-1083 and by AFOSR through Contract # AFOSR-86-0263.

References

1. J. Bardeen, Phys. Rev. 71, 727 (1947),
2. C. J. Sandroff, R. N. Nottenburg, J.-C. Bischoff, and R. Bhat, Appl. Phys. Lett. 57, 33 (1987); E. Yablanovitch, C. J. Sandroff, R. Bhat, and T. Gmitter, Appl. Phys. Lett. 57, 439 (1987).
3. L. G. Meiners and H. H. Wieder, Materials Science Reports, 3, 143 (1988).
4. W. E. Spicer, Z. Liliental-Weber, E. R. Weber, N. Newman, T. Kendelewicz, R. Cao, C. McCants, K. Miyano, P. H. Mahowald and I. Lindau, J. Vac. Sci. and Technol. B6, 1245 (1988).
5. W. E. Spicer, R. Cao, K. Miyano, T. Kendelewicz, I. Lindau, E. Weber, Z. Liliental-Weber and N. Newman, Appl Surf. Sci. 41/42, 1 (1989).
6. E. R. Weber, H. Ennen, V. Kaufmann, J. Windschief, J. Schneider, and T. Wosinski, J. Appl. Phys. 53, 6140 (1982); E. R. Weber and J. Schneider, Physica B 116, 398 (1983).
7. N. Newman, K. K. Chin, W. G. Petro, T. Kendelewicz, M. D. Williams, C. E. McCants, and W. E. Spicer, J. Vac. Sci. Technol. A 3, 996 (1985).
8. N. Newman, W. G. Petro, T. Kendelewicz, S. H. Pan, S. J. Eglash, and W. E. Spicer, J. Appl. Phys. 57, 1247 (1985).
9. N. Newman, W. E. Spicer, and E. R. Weber, J. Vac. Sci. Technol. B 5, 1020 (1987).
10. C. E. McCants, T. Kendelewicz, P. H. Mahowald, K. A. Bertness, M. D. Williams, N. Newman, I. Lindau, and W. E. Spicer, J. Vac. Sci. Technol. A 6, 1466 (1988).
11. Z. Liliental-Weber, N. Newman, J. Washburn, and E. R. Weber, Appl. Phys. Lett. 54, 356 (1989).
12. W. E. Spicer, N. Newman, C. J. Spindt, Z. Liliental-Weber, and E. R. Weber, J. Vac. Sci. and Technol. in press.
13. J. W. Mayer and S. S. Lau, Electronic Materials Science for Integrated Circuits in Si and GaAs, MacMillan, N.Y.; Collier Macmillian, London, 1990 and references therein.

14. J. H. Weaver, in Analysis and Characterization of Thin films, ed. by K. N. Tu and R. Rosenberg (Academic, New York, 1987).

15. C. E. McCants, PhD Dissertation, Stanford University, 1988 unpublished, p. 38.

16. M. W. Ruckman, M. del Giudice, J. J. Joyce, and J. H. Weaver, Phys. Rev. B 33, 2191 (1987); R. Ludeke and G. Landgren, Phys. Rev. B 33, 5526 (1986).

17. J. Nogami, T. Kendelewicz, I. Lindau, and W. E. Spicer, Phys. Rev. B 34, 669 (1986).

18. T. Kendelewicz, M. D. Williams, W. G. Petro, I. Lindau, and W. E. Spicer, Phys. Rev. B 32, 3758 (1985).

19. W. G. Petro, I. A. Babalola, T. Kendelewicz, I. Lindau, and W. E. Spicer, J. Vac. Sci. Technol. A1, 1181 (1983).

20. S. H. Pan, T. Kendelewicz, W. G. Petro, M. D. Williams, I. Lindau, and W. E. Spicer, Mat. Res. Soc. Symp. Vol. 25, J. E. Gablin, ed., North-Holland, N.Y. (1984) 335.

21. M. D. Williams, T. Kendelewicz, N. Newman, I. Lindau, and W. E. Spicer, J. Vac. Sci. Technol. A3, 977 (1985); T. Kendelewicz, W. G. Petro, S. H. Pan, M. D Williams, I. Lindau, and W. E. Spicer, Appl. Phys. Lett. 44, 113 (1984).

22. R. Ludeke, T. C. Chiang, and T. Miller, J. Vac. Sci. Technol. B 1, 581 (1983).

23. J. W. Mayer and S. S. Lau, Electronic Materials Science for Integrated Circuits in Si and GaAs, MacMillan, N.Y.; Collier Macmillian, London, 1990, p. 301.

24. P. Skeath, C. Y. Su, I. Lindau, and W. E. Spicer, J. Vac. Sci. Technol. 17, 874 (1990; J. Vac. Sci. Technol. 19, 556 (1981); C. B. Duke, A. Paton, L. J. Brillson, A. Kahn, D. Kanani, J. Carelli, G. Margaritondo, and A. Katnani, Phys. Rev. Lett. 46, 440 (1981; R. Z. Bachrach, and R. S. Bauer, J. Vac. Sci. Technol. 16, 1149 (1979); A. Kahn, J. Carelli, K. Kanani, C. B. Duke, A. Paton, and L. J. Brillson, J. Vac. Sci. Technol. 19, 331 (1981).

25. F.Xu, Z. Lin, D. M. Hill, J. H. Weaver, Phys. Rev. 36, 6624 (1987); C. E. McCants, T. Kendelewicz, P. H. Mahowald, K. A. Bertness, M. D. Williams, N. Newman, I. LIndau, and W. E. spicer, J. Vac. Sci. Technol. A6 1466 (1987); C. E. McCants, PhD dissertation 1988, unpublished.
26. Metallization and Metal-Semiconductor Interfaces, NATO ASI Series, Series B, Physics 195, ed. I. B. Batra, Plenum Press, NY and London, 1989.
27. V. Heine, Phys. Rev. A 138 1689 (1965); G. Louie and M. L. Cohen, Phys. Rev. B 13, 2461 (1976); C. Tejedor, F. Flores, and E. Louis, J. Phys. C. (Solid State Physics) 10, 2163 (1977); J. Tersoff, Phys. Rev. Lett. 52, 465 (1984).
28. Metal-Semiconductor Contacts, E. H. Rhoderick and R. J. Williams, Clarendon Press, Oxford, 1988.
29. L. J. Brillson and P. Chiaradia, Metallization and Metal-Semiconductor Interfaces, NATO ASI Series, Series B, Physics 195, ed. I. B. Batra, Plenum Press, NY and London, 1989, p. 91
30. W. E. Spicer, P. W. Chye, P. R. Skeath, C. Y. Su and I. Lindau, J. Vac. Sci. Technol. 16, (1979) 1427; 17 1019 (1980); Phys. Rev. Lett. 44 420 (1980).
31. W. E. Spicer, Metallization and Metal-Semiconductor Interfaces, NATO ASI Series, Series B, Physics 195, ed. I. B. Batra, Plenum Press, NY and London, 1989, p. 139.
32. J. L. Freeouf and J. M. Woodall, Appl. Phys. Lett 39, 727 (1981).
33. R. Ludeke, Metallization and Metal-Semiconductor Interfaces, NATO ASI Series, Series B, Physics 195, ed. I. B. Batra, Plenum Press, NY and London, 1989, p. 39.
34. J. Tersoff, Phys. Rev. Lett. 52, 465 (1984).
35. S. B. Zhang, M. L. Cohen, and S. B. Louie, Phys. Rev. B 32, 3955 (1985).
36. R. E. Allen and J. D. Dow, Phys. Rev. B 25, 1423 (1982).
37. E. R. Weber, H. Ennen, V. Kaufmann, J. Windscheif, J. Schneider, and T. Wosinski, J. Appl. Phys. 53 (1982) 6140; E. R. Weber and J. Schneider, Physica 116B (1983) 398.

38. W. Mönch, in: Chemistry and Physics of Solid Surfaces, Vol. V, Eds. R. Vanselow and R. Howe (Springer, Berlin, 1984) p. 501.
39. W. Mönch and H. Gant, Physica 117/118 (1983) 801.
40. N. Newman, W. E. Spicer, and E. R. Weber, J. Vac. Sci. Technol. B 5, 1020 (1987).
41. W. E. Spicer, T. Kendelewicz, N. Newman, R. Cao, C. McCants, K. Miyano, I. Lindau, and E. R. Weber, Appl. Surf. Science, 33/34, 1009 (1988).
42. E. R. Weber, W. E. Spicer, N. Newman, Z. Liliental-Weber, T. Kendelewicz, Proc. 19th Internal. conf. on Phys. Semicond. Warsaw, 1988 (in press).
43. Hurle gives a good discussion for melt, LPE- and VPE-grown material. MBE is grown under As rich conditions. See D. T. J. Hurle, in Proc. Conf. on Semi-Insulating III-V Materials, Malmo, (1988) in press.
44. G. Baraff and M. Schluter, Phys. Rev. Lett. 55, 1327 (1987);
45. G. A. Baraff and M. Schluter, Phys. Rev. B 35, 6154 (1987).
46. F. Bartels, H. J. Clements, and W. Mönch, Physica 117B and 118B, 801-803 (1983).
47. G. M. Martin, J. P. Farges, G. Jacob, J. P. Hallais, J. Appl. Phys. 51, 2840 (1980).
48. C. D. Thurmund, G. P. Schwartz, G. W. Kammlott, and B. Schwartz, J. Electrochemical Soc. 127, 1367 (1980).
49. A. Zur, T. C. McGill, and D. Z. Smith, J. Vac. Sci. and Technol. B1, 608 (1983).
50. J. R. Waldrop, J. Vac. Sci. Technol. B 2, 445 (1984).
51. K. Miyano, D. King, C. J. Spindt, T. Kendelewicz, R. Cao, Z. Yu, I. Lindau, and W. E. Spicer, in preparation.
52. Charles Kittel, Introduction to Solid State Physics - 6th ed., Wiley, 1986.
53. R. Z. Bachrach, R. S. Bauer, P. Chiaradia, and G. V. Hansson, J. Vac. Sci. Technol. 19, 335 (1981).

54. S. P. Svensson, J. Kanski, T. G. Anderson, and P. O. Nilsson, J. Vac. Sci. Technol. B 2, 335 (1981).
55. T. Yokotsuka, T. Narusawa, Y. Uchida, and H. Nakashima, Appl. Phys. Lett. 50 (1987) 591; Y. Uchida, T. Yokotsuka, H. Nakashima, and S. Takatani, Appl. Phys. Lett. 50 (1987) 670.
56. J. R. Waldrop and R. W. Grant, Appl. Phys. Lett. 50, 250 (1987).
57. R. W. Grant and J. R. Waldrop, J. Vac. Sci. and Technol. B 5, 1015 (1987).
58. P. Chiaradia, A. D. Katnani, H. W. Sang, Jr., and R. S. Bauer, Phys. Rev. Lett. 52, 1246 (1984).
59. W. E. Spicer, I. Lindau, P. E. Gregory, C. M. Garner, P. Pianetta, and P. W. Chye, J. Vac. Sci. Technol. 13, 780 (1976); J. van Laar and A Huijser, J. Vac. Sci. Technol. 13 769 (1976).
60. W. Mönch, R. S. Bauer, H. Gant, and R. Marshall, J. Vac. Sci. and Technol. 21, 498 (1982).
61. P. H. Mahowald and W. E. Spicer, J. Vac. Sci. Technol. B 6, 1539 (1988).
62. P. H. Mahowald, Ph.D. dissertation, Stanford University, 1987 (unpublished).
63. P. H. Mahowald, T. Kendelewicz, K. A. Bertness, C. E. McCants, M. D. Williams, and W. E. Spicer, J. Vac. Sci. Technol. B 5, 1258 (1987).
64. E. b. Marshall, S. S. Lau, C. J. Pamstrom, T. Sands, C. L. Schwartz, S. A. Swartz, and J. P. Harbison, and L. T. Florez, Mat. Res. Soc. Symposium Proceedings, 148, 163 (1989); S. S. Lau et al. Mat. Res. Soc. Symposium, Spring 1990.
65. E. B. Marshall, B. Zang, L. C. Wang, P. F. Jiao, W. X. Chen, T. Sawada, and S. S. Lau, J. Appl. Phys. 62, 942 (1987).
66. Renyu, Cao, Ph. D. Dissertation, Stanford University, 1989 (unpublished); the Ga data can also be found in Ref (5) and Ref. (27).
67. D. Bolmont, P. Chen, and C. A. Sebenne, P. Chen, Sur. Sci. 117, 417 (1982).
68. S. P. Svensson, J. Kanski, and G. Anderson, Phys. Rev. B 30, 6033 (1984).

69. D. J. Stirland, M. R. Brazel, and I. Grant, Appl. Phys. Lett. 46, 1066 (1985).
70. Z. Liliental-Weber, J. Vac. Sci. Technol. B 5, 1007 (1987); and ref. therein.
71. Z. Liliental-Weber, E. R. Weber, N. Newman, W. E. Spicer, R. Gronsky, and J. Washburn, in Defects in Semiconductors, ed. J. van Bardeleban, Materials Science Forum, 10-12 (1986) pp. 1223-1228.
72. J. B. Pallix, C. H. Becker, N. Newman, MRS Bulletin 12, 52 (1987).
73. C. H. Becker and K. T. Gillen, Anal. Chem. 56, 1671 (1984); J. Vac. Sci. Technol. A 3, 1347 (1985).
74. H. H. Wieder, BLSI Electronics Microstructure, 10, ed. by N. G. Einspruch and R. S. Bauer, Academic Press, London, 1985, p. 201; C. D. Thurmond, G. P. Schwartz, J. Electrochemical Soc. 127, 1367 (1980); W. E. Spicer, I. Lindau, P. Skeath, and C. Y. Su, J. Vac. Sci. Technol. 17, 1019 (1980) and ref. therein.
75. Q.-D. Qian, M. R. Melloch, J. A. Cooper, L. A. Kolodziejski, M. Kobayashi, and R. L. Gunshor, Appl. Phys. Lett. 54, 1359 (1989).
76. G. G. Fountain, S. V. Hatangady, R. A. Rudder, R. J. Markunas, G. Lucovsky, S. S. Kim, and D. V. Tsu, J. Vac. Sci. Technol. A7, 576 (1989).
77. E. Yablanovitch, C. J. Sandroff, R. Bhat, and T. Omitter, Appl. Phys. Lett. 51, 439 (1987); C. J. Sandroff, R. N. Nottenburg, J-C, Bischoff, and R. Bhat, Appl. Phys. Lett. 51, 439 (1987).
78. C. J. Spindt and W. E. Spicer, Journal of Elect. Chem. Soc. in press.
79. R. S. Besser and C. R. Helms, Appl. Phys. Lett. 52, 1707 (1988); J. Appl. Phys. 65, 4306 (1989).
80. D. Liu, T. Zhang, R. A. LaRue, J. S. Harris, Jr. and T. W. Sigmon, Appl. Phys. Lett. 53, 1059 (1988).
81. D. Liu, E. C. Larkins, T. Zhang, T. T. Chiang, R. A. LaRue, T. Sigmon, W. E. Spicer, and J. S. Harris, Jr., Proceedings of the 15th International Symposium on

GaAs and Related Compounds, Atlanta, GA, Institute of Physics, Bristol, England (1988).

82. H. Hasegawa, H. Ishii, T. Sawada, T. Saitoh, S. Knoishi, Y. Liu, and H. Ohno, J. Vac. Sci. Technol. B 6 1184 (1988).
83. C. J. Spindt, R. S. Besser, R. Cao, K. Miyano, C. R. Helms and W. E. Spicer, Appl. Phys. Lett. 54, 1148 (1989); C. J. Spindt, D. Liu, K. Miyano, P. Meissner, T. T. Chiang, T. Kendelewicz, I. Lindau, and W. E. Spicer, Appl. Phys. Lett. 55, #9 (1989).
84. C. J. Spindt and W. E. Spicer, Appl. Phys. Lett. 55, 1653 (1990).
85. R. Besser Ph.D dissertation, Stanford University, unpublished.

Table I: Fermi level Motion and Metal/GaAs Interfacial Chemistry

Metal	Fermi Level (E_f) Position Before Anneal	Fermi Level (E_f) Position After Anneal	E_f Movement with respect to VBM	Interfacial Chemistry Expected for Annealing	Reaction Product (As or Ga)
Ag	0.5	0.5	none	none	none
Au	0.5	0.6	+0.1	Au + GaAs -> AuGa + As	As
Al	0.65	0.55	-0.1	Al + GaAs -> AlAs + Ga	Ga
Ti	0.7	0.6	-0.1	Ti + GaAs -> TiAs +Ga	Ga
Cr	0.75	0.75	none	Cr + GaAs -> GaCr + CrAs	neither

Table II: Various Reports of the Electrical Characteristics of Ga Contacts on GaAs

- Ohmic contact on p-GaAs

R. Z. Bachrach and A. Bianconi, J. Vac. Sci. Technol. 15, 525 (1978).

- Ohmic contact on n-GaAs

J. Woodall and C. Lauza, J. Vac. Sci. Technol. 15, 1436 (1978).

- 1.05 eV Schottky barrier height on MBE, As Rich, (100) n-GaAs for thick Ga layers

S. P. Svensson, J. Kanski, and G. Anderson, Phys. Rev. B 30, 6033 (1984).

- 1.15-1.2 eV Schottky barrier height for electrochemical metal depositons on n-GaAs:

Related to metallic Ga which they believe is formed

R. Reinke and Meming, Surf. Sci. 192, 66 (1987).

- 1.0-1.1 eV Schottky barrier height for thick Ga on GaAs (110)

A. B. McLean and R. H. Williams, Semicond. Sci. Technol. 21, 654 (1987).

A summary of published results on Ga/GaAs contacts

By comparison with other metals of comparable electronegativity, one would expect a barrier height of only about 0.8 eV on n-GaAs [Ref. 69]. In contrat the reported barrier heights are about 1.1 eV. This is higher than those reported for any other metal.

Table III: Arsenic Excess at the Schottky Barrier Interface and Changes with Annealing

Metal	As Excess after Metal Deposition EDX Result	Changes in As Excess Due to Annealing		Direction of Movement of Fermi Level	
		Predicted	Observed	Predicted	Observed
Au	Yes	Increase	Increase	Toward CBM	Toward CBM
Al	Yes	Decrease	Decrease	Toward VBM	Toward VBM
Cr	Yes	none	none	none	none
$TiSi_2$	Yes	not done		not done	

Figure Captions

Figure 1 I-V data from the thick-film:n-type-GaAs diode. All measurements were performed at room temperature after annealing at various temperatures. The barrier height and ideality factor are determined from the following equation ($I = SA^{*} T^{2} e^{-\Phi_b/V_t} (e^{V-IR/nV_t} - 1)$).

Figure 2 I-V data from the thick-film Al:n-type-GaAs(110) diode. These diodes were fabricated on a clean cleaved GaAs(110) surface under UHV conditions. All measurements were performed at room temperature after annealing to various temperatures. The barrier height is determined from the equation in Fig. 1. It is a measure of the energy separation between the E_{fi} and the CBM at the interface.

Figure 3 Relationship between E_{fi} position and Schottky barrier heights on n- and p-semiconductors. E_{fi} is measured from the VBM. See equations (1) and (2) in the text.

Figure 4 Experimentally obtained elastic scattering lengths in various solids. Data points 1 through 28 see *Lindau and Spicer 1974*; 29 and 30 from *Evans, Pritchard and Thomas 1979*; 31 from *Jacobi and Hölzl 1971*; "Our Work" is derived from carbon 1*s* surface core level shifts of diamond (111) 2 x 2/2 x 1 as described in Section 1.7.

Figure 5a (1) As 3d core level spectra for the room temperature Ti/GaAs (110) interface. The dots represent the raw data, the solid line through the dots is the curve fit to the data, and the various components are labeled according to the shading: the wide cross hatching represents the surface shifted component, the light and dark cross hatchings represent the reacted components, and no shading represents the substrate component. Photon energy is equal to 70 eV.

(2) Ga 3d core level spectra for the room temperature Ti/GaAs(110) interface. The dots represent the raw data, the solid line through the dots is the curve fit to the data, and the various components are labeled according to the shading: the cross hatching represents the surface shifted component, the solid shading represents the reacted component, and no shading represents the substrate component. Photon energy is 50 eV.

Figure 5b (1) As 3d core level spectra for the room temperature Ti/GaAs(110) interface for higher Ti coverages.

(2) Ga 3d core level spectra for the room temperature Ti/GaAs(110) interface for higher Ti coverages. No emission is observed for coverages higher than 17.3 ML.

Figure 6 Chemistry or lack thereof due to noble and transition metals on GaAs as seen through the Ga and As 3d levels.

Figure 7 Energy level diagram for the Antisite Defect Model (ADM). The As_{Ga} antisite double donor with levels of 0.76 and 0.5 eV and the compensating acceptor (probably the Ga_{As} antisite) with energy levels below 0.5 eV are shown. Both defects are located in the same spatial region near the surface. The surface Fermi level position, E_f, for the free surface will be determined by the relative densities of the two defects in the near surface region. In the usual case where $E_{fi} > 0.5$ eV, the density of $As_{Ga} > Ga_{As}$.

Figure 8 The diagram to the left is taken from Ref. 30. This energy level diagram indicates the pinning positions obtained on n- and p-GaAs with very low coverages (order 1 ML or less) of the indicated element measured at room temperature (E_g - 1.42 eV). The pinning positions are identical within experimental error to those obtained in the present work for Al, Ga, In, and Sb. The vertical lines through those data points indicate defect energy levels deduced in 1979. The right diagram indicates the energy of the As_{Ga} antisite levels from the VBM measured at 8 K (E_g = 1.52 eV) by Weber et al. in 1982 [37]. As can be seen, the two sets of levels are found to agree.

Figure 9 The surface E_f of the free (100) surface grown by MBE for n-type and p-type GaAs. The three surface reconstructions are indicated on the horizontal axis. All the surfaces are As rich with the amount of excess As increasing from (4x6) to C(4x4). The energy levels of the AUDM model are shown. Note that these are the same as the pinning levels found on cleaved GaAs(110) surfaces due to metal or non-metal depositions.

Figure 10 Surface or Interrace Fermi level position, E_{fi} for LaB_6 on GaAs.

Upper panel - The Ga 2p core level position on MBE (100) GaAs due to LaB_6 deposition and/or annealing. The left hand scale was obtained by assuming a 0.9 eV position after annealing. The arrows (1), (2) and (3) indicate changes due to LaB_6 deposition on different starting surfaces.

Lower panel - The Schottky barrier heights as a function of annealing for 1800Å or LaB_6 on GaAs. Open circles indicate MBE and closed circles chemically etched (100) GaAs surfaces.

Figure 11 Summary of several E_f^i measurements. Overlayer characteristics are given at bottom of figure. Unless noted otherwise, overlayer thicknesses are nominally ~ 10 Å and depositions intended to incorporate As or P in the overlayer were carried out in 10^{-7}

Torr background pressure of As_4 or P_2: (a) Ge overlayers deposited in vacuum; (b) Ge overlayers deposited in As_4; (c) Ge overlayers initially deposited in vacuum but completed with deposition in P_2; (d) Ge overlayer deposited in P_2; (e) Si overlayer deposited in As_4.

Figure 12 Representative I-V data for a selection of contacts to GaAs that have a variety of structures (contact area = 5.07×10^{-4} cm^2). Multilayered contact structures are shown schematically on the right.

Figure 13 Fermi level movement due to adding Ge along to the surface. The greater the amount of excess As in the surface (see text), the greater the Fermi level movement.

Figure 14 Schematic of the energy bands and the Fermi-level position at the interface on a 10-Å scale. The valence-band discontinuity is the same at the interface between the various surface reconstructions of GaAs(100) surface and Ge. However, the Fermi level position at the interface depends on the surface stoichiometry. This observation clearly demonstrates the independence of the interfacial Fermi level and the valence-band discontinuity.

Figure 15 The evolution of the Fermi level during the interface formation with Ge. The difference between this figure and Fig. 13 is that Ge is deposited with As. As source was open. The figure when compared with Fig. 13 shows that the presence of As influences the final E_F position E_F for the Ga-rich, (4x6) surfaces moved toward the conduction band by over 0.10 eV. E_F for the As-rich, c(4x4) only slightly moved toward the conduction band because E_F is already close to the top of the Ge conduction band in Fig. 13 (Ref. 61).

Figure 16 An explanation of Fermi level motion in terms of the Antisite Defect Model. The upper and lower panels give band diagrams before and after adding a n-doped Ge overlayer and strong n-doping of the GaAs adjacent to the interface. The Fermi level moves upward due to the interfacial states near mid-gap being filled by electrons from the new depleted region and the n-doped Ge. For simplicity the band bending in the upper panel is not shown. The lower panel shows schematically the change in band bending.

Figure 17 The data (dots and heavy solid line) for the Ge/InP Fermi energy is shown above. The shaded line is the model evaluated with the donor and acceptor energies appropriate for InP (1.1 and 0.9 eV from the VBM). The defect density is 3 x 10^{13} cm^{-2} $Å^{-1}$ (same as for GaAs) and the doping donor density is 10^{13} cm^{-2} $Å^{-1}$. These values were chosen to fit the data.

Figure 18 The Pd/Ge/GaAs ohmic contact. The upper panel shows the locations of the various parts of this contact. The middle panel gives a schematic of the contact resistivity data of Lau et al. This indicates a barrier height of about 0.3 eV. The lower panel indicates the suggested band diagram for this contact.

Figure 19 SALI analysis of Pallix, Becker, and Newman [75] for 1000Å of Au on GaAs. Note in particular the region at the Au/GaAs interface. The upper panel gives the results for an unannealed sample. There is little As or Ga in the Au. Panel (b) gives the results after thermal annealing. The most striking change is the large increase in As as the sputtering approaches the Au/GaAs interface (indicated by the arrow). Ga and, to a less extent, As are also seen in the Au and at the outside surface.

Fugure 20 Results for the Fermi level position as a function of sulfur treatment. Surface Fermi level position (labeled "Surface Potential" in the figure) of GaAs after various treatments as obtained by Besser and Helms (see Ref. 79). As can be seen the Na_2S and $(NH_4)_2S$ treatments move the Fermi level toward the valence band, i.e. increase the band bending rather than produce flat band conditions).

Figure 21 Changes in band bending and Fermi level position due to sulfur treatment. Note that the treatment produces about 0.2 eV increase in band bending. An explanation of this in terms of the ADM is also shown. A decrease in the number of As_{Ga} relative to Ga_{As} antisites moves E_f to near the lower As_{Ga} level at 0.5 eV. This inhibits surface recombinations by increasing the band bending and charging the As_{Ga} recombination centers positively so that it will repel electrons.

Figure 22 Surface DLTS for (100) GaAs after Liu et al. (Ref. 82). The untreated sample shows a trap at about 0.85 eV (dashed curve). In the treated sample (solid curve) the 310 K signal disappeared and a new, weaker signal at about 0.3 eV above the VBM was found

Figure 1

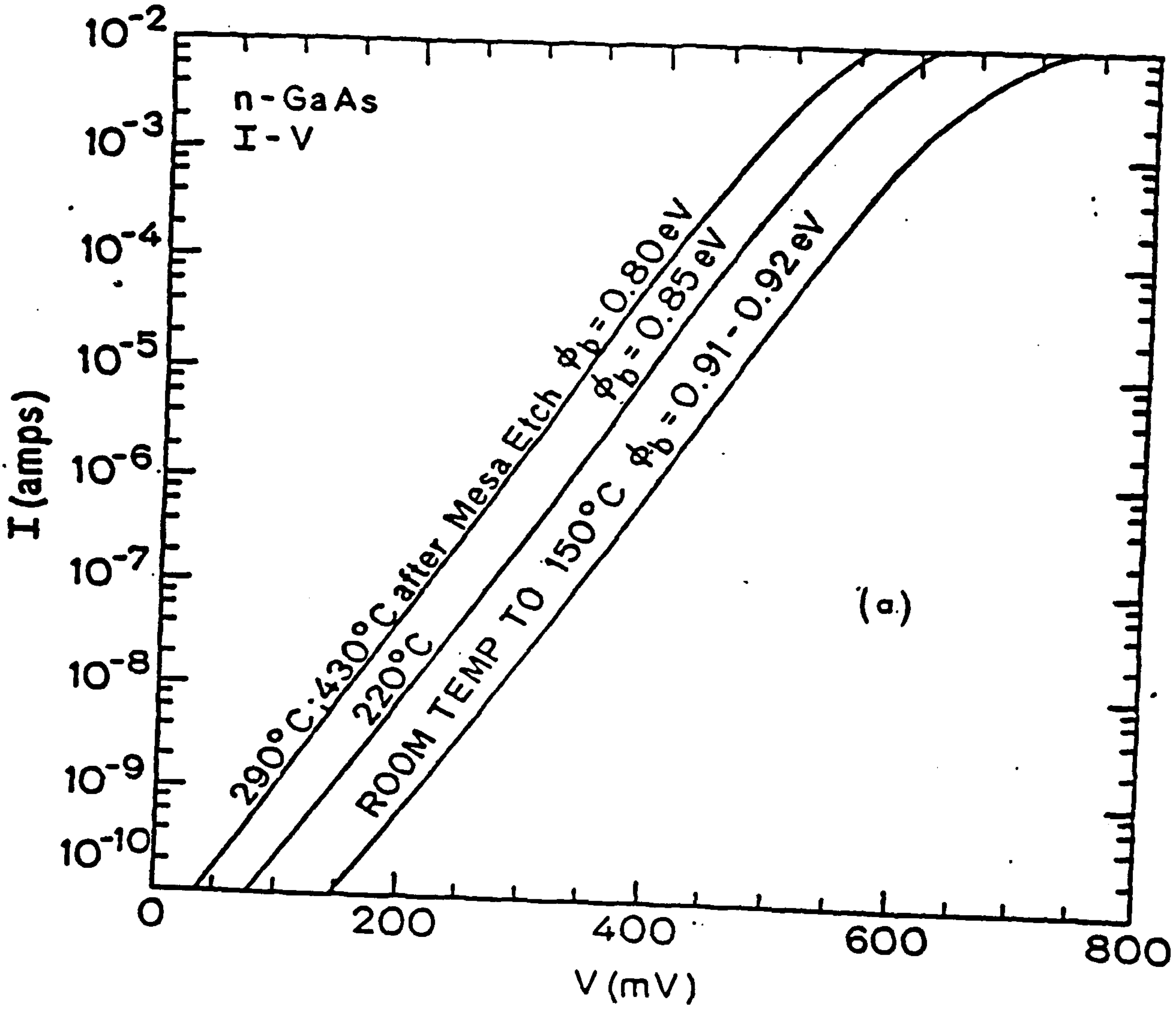

n-GaAs
I-V
$\phi_b = 0.80$ eV
290°C : 430°C after Mesa Etch
$\phi_b = 0.85$ eV
220°C
$\phi_b = 0.91 - 0.92$ eV
ROOM TEMP TO 150°C
(a)
I (amps)
10^{-2}
10^{-3}
10^{-4}
10^{-5}
10^{-6}
10^{-7}
10^{-8}
10^{-9}
10^{-10}
0
200
400
600
800
V (mV)

Figure 2

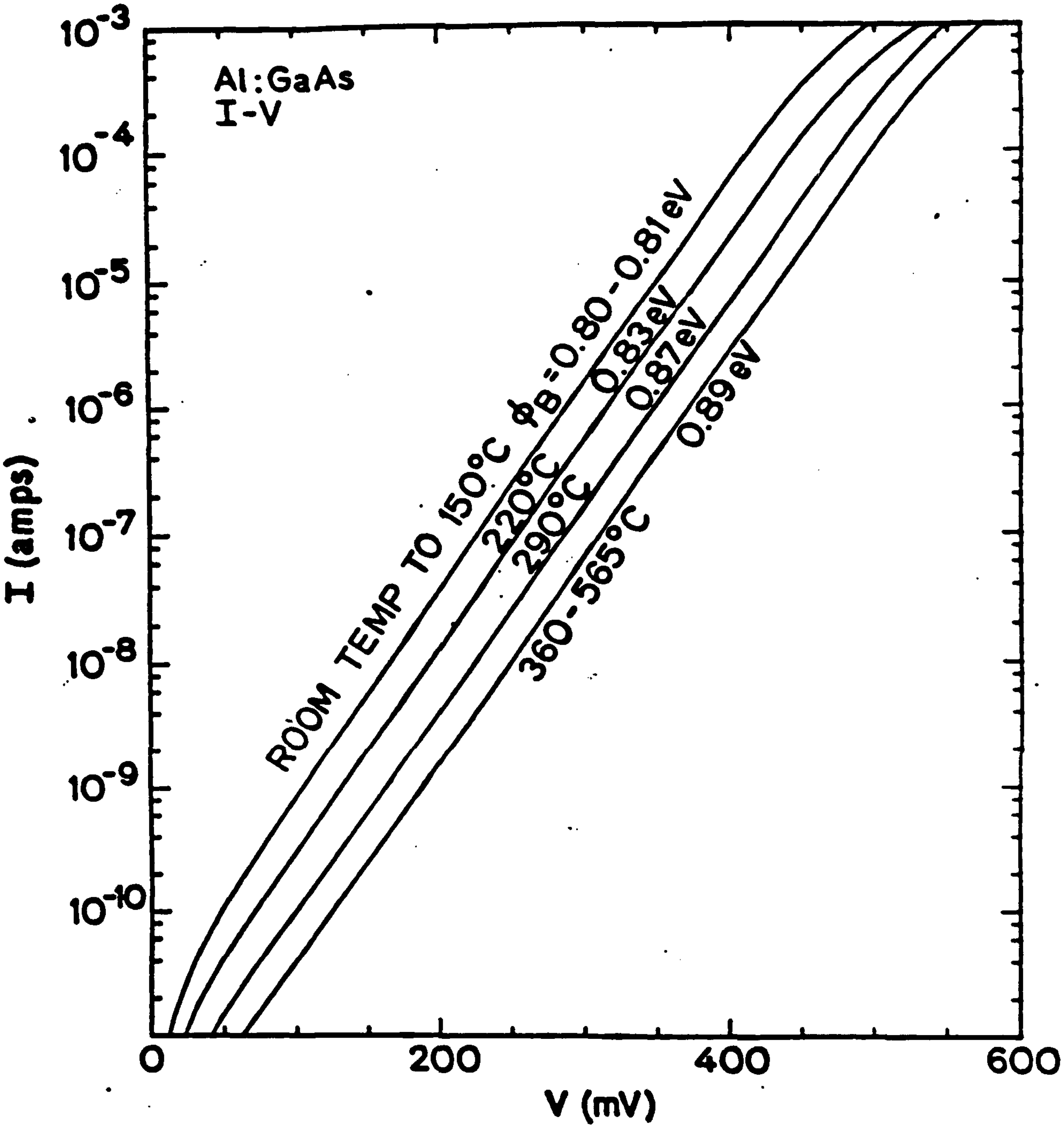
Al:GaAs
I-V
ROOM TEMP TO 150°C ϕ_B=0.80-0.81eV
220°C 0.83eV
290°C 0.87eV
360-565°C 0.89eV
I (amps)
10^{-3}
10^{-4}
10^{-5}
10^{-6}
10^{-7}
10^{-8}
10^{-9}
10^{-10}
0
200
400
600
V (mV)

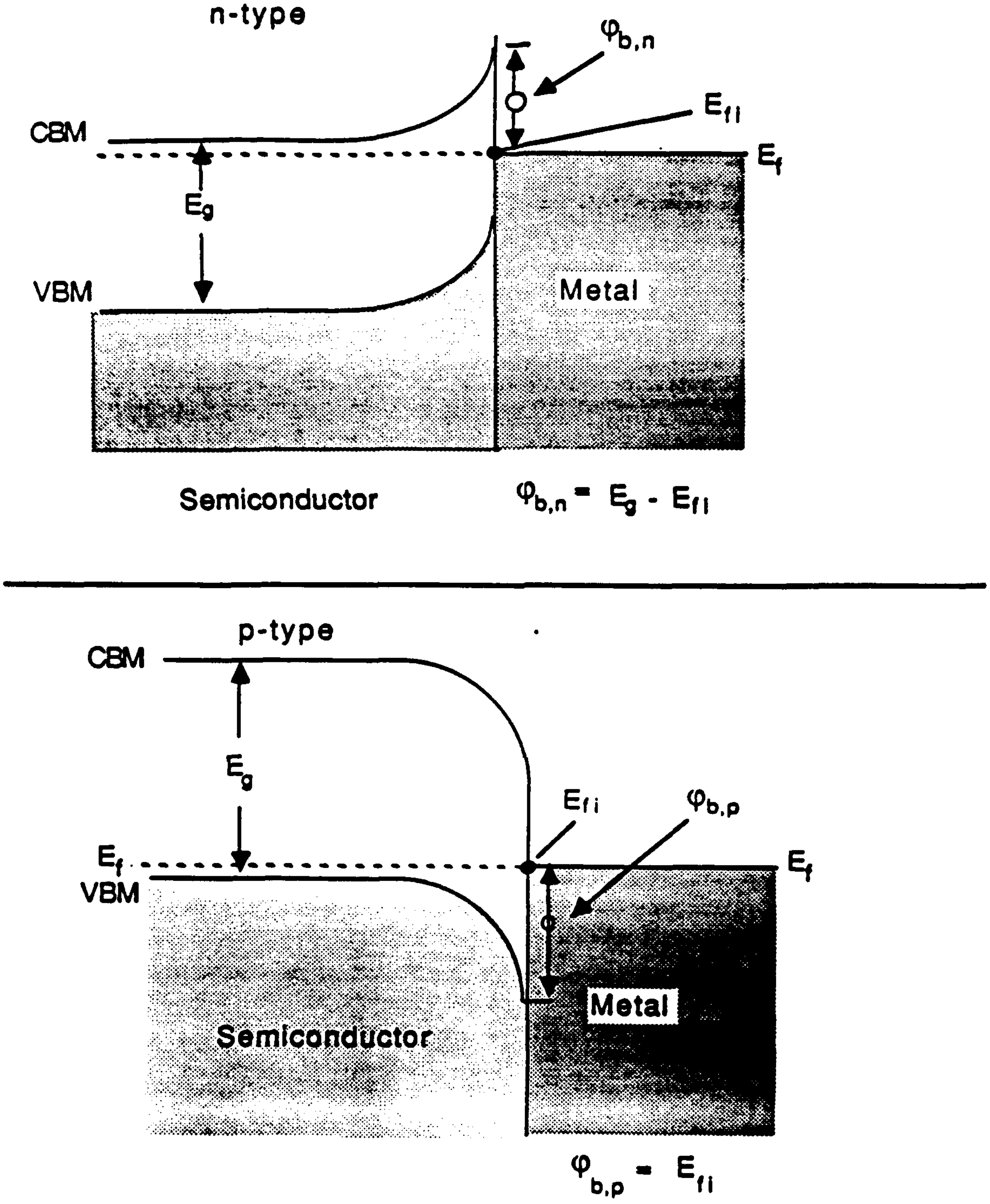

where: $\varphi_{b,n}$ = Schottky Barrier Height on n-type

$\varphi_{b,p}$ = Schottky Barrier Height on p-type

E_{fi} = position of Fermi level at interface (same on n- and p-type)

and $\varphi_{b,n} + \varphi_{b,p} = E_g$

Figure 3

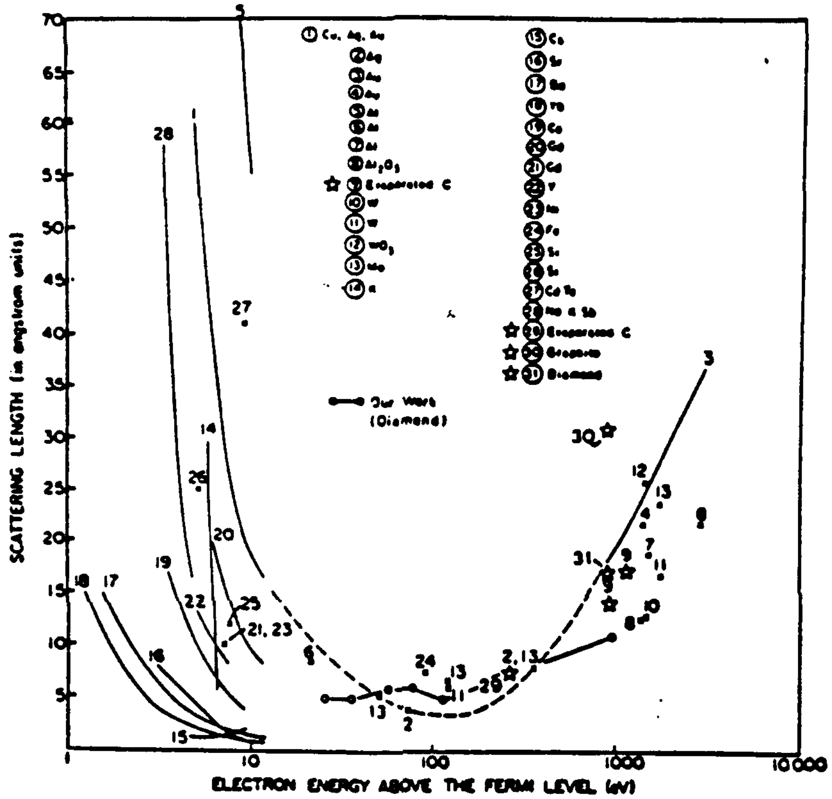

SCATTERING LENGTH (in angstrom units)
70
65
60
55
50
45
40
35
30
25
20
15
10
5
ELECTRON ENERGY ABOVE THE FERMI LEVEL (eV)
1
10
100
1000
10000
① Cu, Ag, Au
② Ag
③ Au
④ Au
⑤ Al
⑥ Al
⑦ Al
⑧ Al2O3
☆ ⑨ Evaporated C
⑩ W
⑪ W
⑫ WO3
⑬ Mo
⑭ C
⑮ Cs
⑯ Sr
⑰ Ba
⑱ Yb
⑲ Ca
⑳ Ge
㉑ Gd
㉒ V
㉓ Ni
㉔ Fe
㉕ Sc
㉖ Si
㉗ Cs Te
㉘ Na & Sb
☆ ㉙ Evaporated C
☆ ㉚ Graphite
☆ ㉛ Diamond
Our Work (Diamond)
5
28
1
27
14
26
20
19
22
25
21, 23
18
17
16
15
6
24
13
13
2
11
2, 13
29
3
30
12
13
4
31
9
7
11
8
10
8

Figure 4

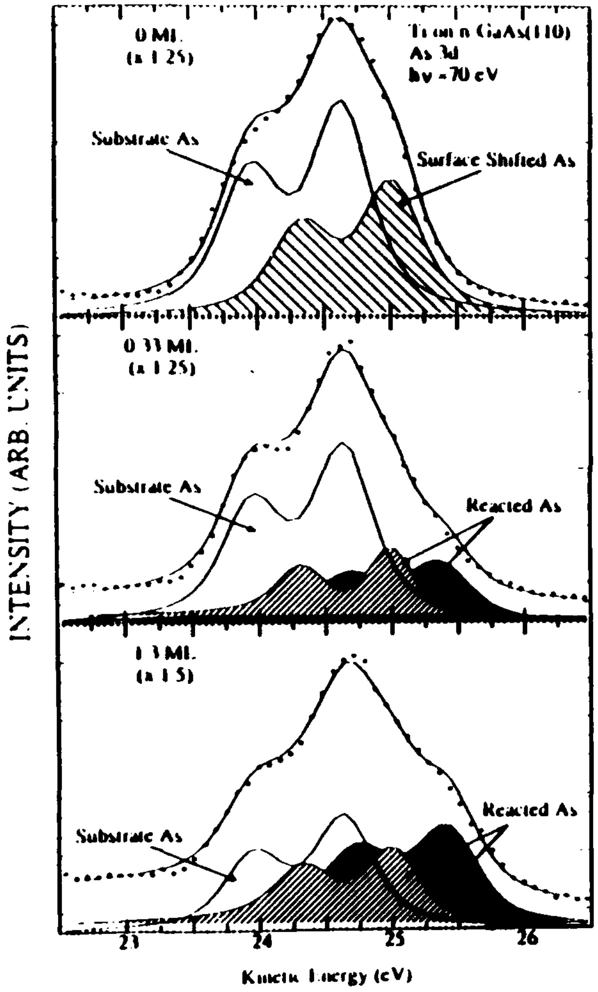
INTENSITY (ARB. UNITS)
0 ML
(x 1.25)
Ti on n GaAs(110)
As 3d
hν = 70 eV
Substrate As
Surface Shifted As
0.33 ML
(x 1.25)
Substrate As
Reacted As
1.3 ML
(x 1.5)
Substrate As
Reacted As
23
24
25
26
Kinetic Energy (eV)

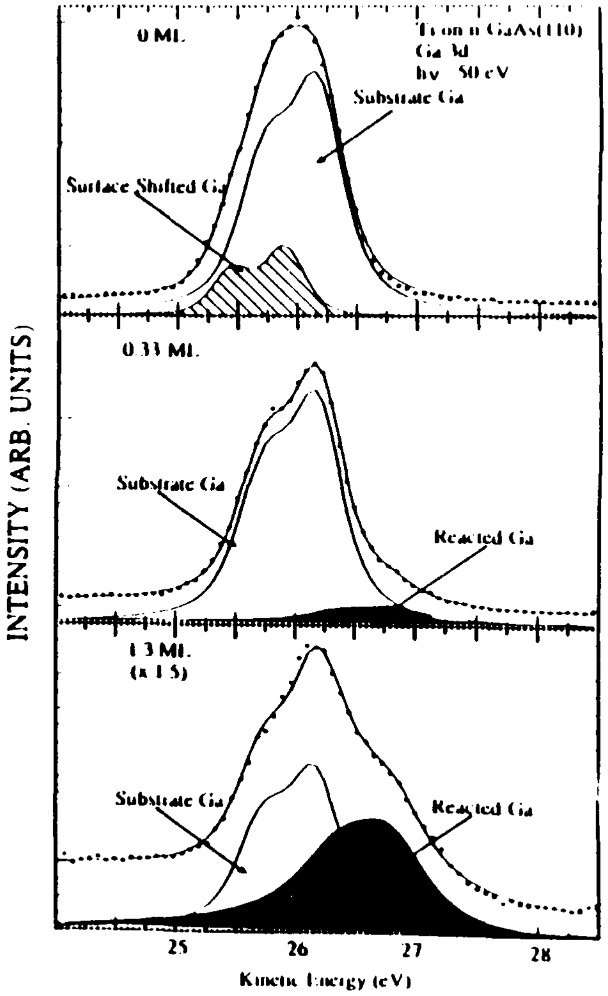
INTENSITY (ARB. UNITS)
0 ML
Ti on n GaAs(110)
Ga 3d
hν = 50 eV
Substrate Ga
Surface Shifted Ga
0.33 ML
Substrate Ga
Reacted Ga
1.3 ML
(x 1.5)
Substrate Ga
Reacted Ga
25
26
27
28
Kinetic Energy (eV)

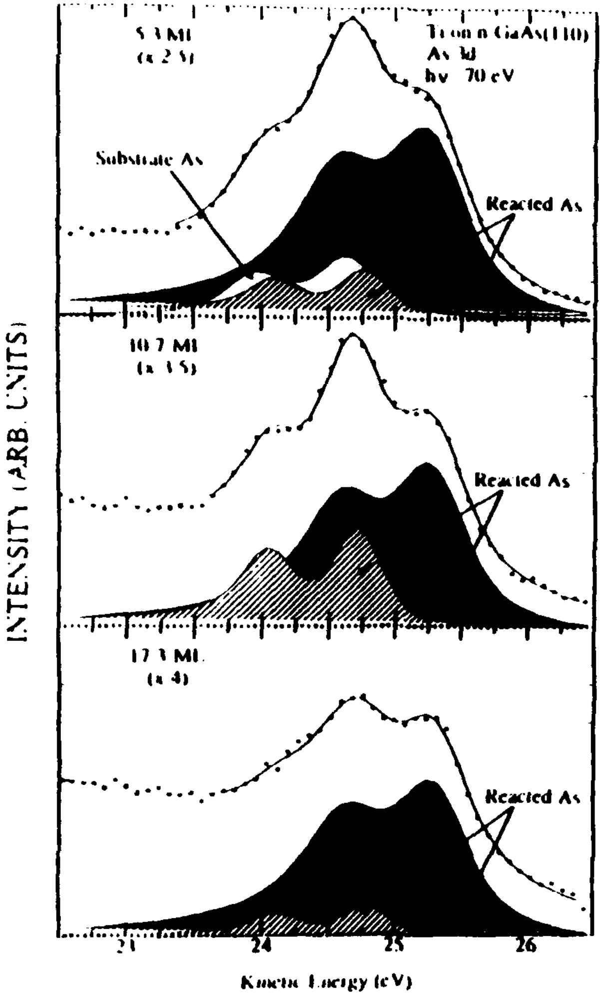

Ti on n GaAs(110)
As 3d
hv 70 eV
5.3 ML
(x 2.5)
Substrate As
Reacted As
10.7 ML
(x 3.5)
Reacted As
17.3 ML
(x 4)
Reacted As
INTENSITY (ARB. UNITS)
23
24
25
26
Kinetic Energy (eV)

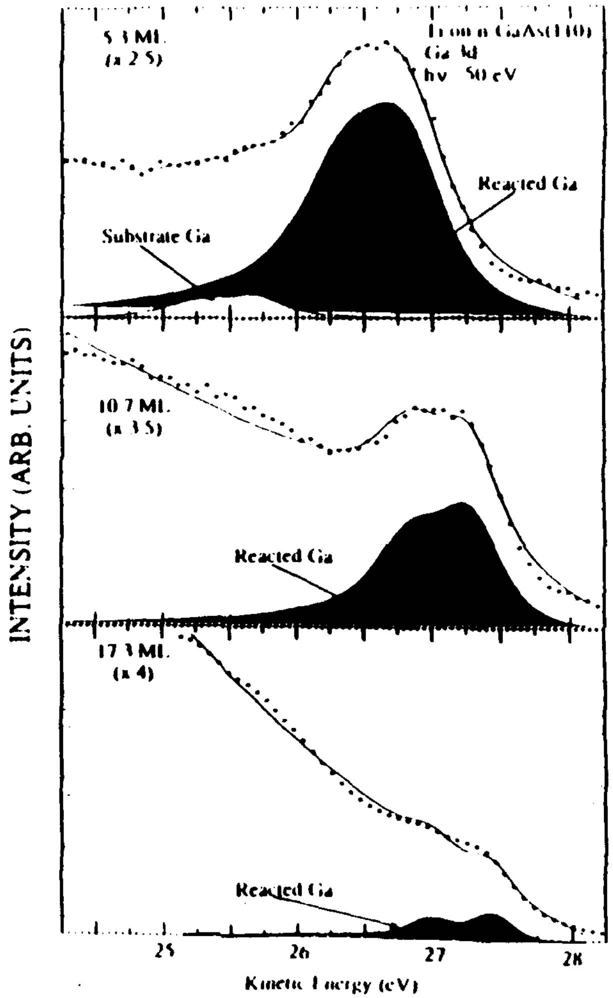

Ti on n GaAs(110)
Ga 3d
hv 50 eV
5.3 ML
(x 2.5)
Reacted Ga
Substrate Ga
10.7 ML
(x 3.5)
Reacted Ga
17.3 ML
(x 4)
Reacted Ga
INTENSITY (ARB. UNITS)
25
26
27
28
Kinetic Energy (eV)

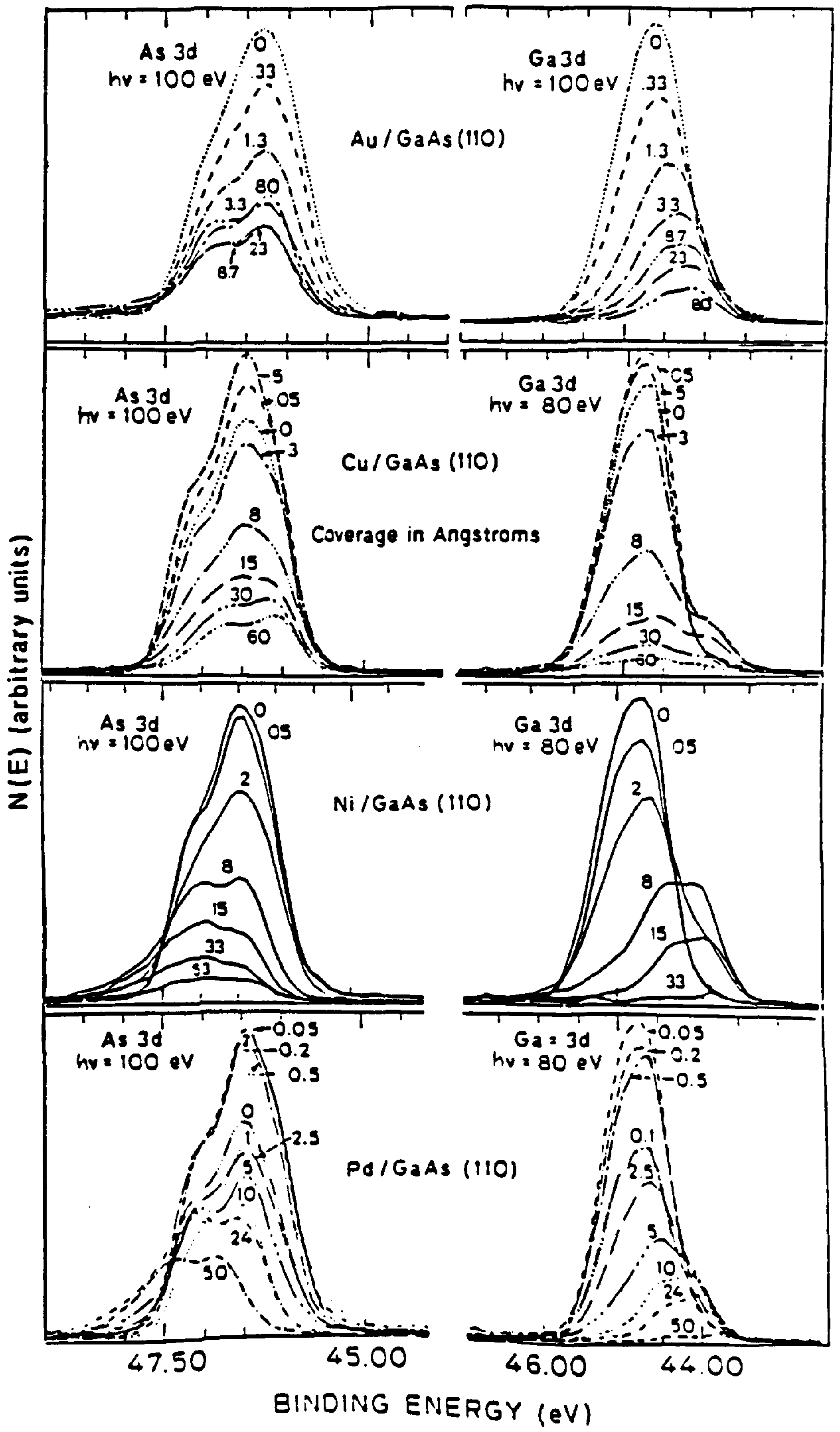
As 3d
hv = 100 eV
Ga 3d
hv = 100 eV
Au / GaAs (110)
0
.33
1.3
3.3
80
8.7
23
As 3d
hv = 100 eV
Ga 3d
hv = 80 eV
Cu / GaAs (110)
Coverage in Angstroms
5
.05
0
3
8
15
30
60
As 3d
hv = 100 eV
Ga 3d
hv = 80 eV
Ni / GaAs (110)
0
.05
2
8
15
33
93
As 3d
hv = 100 eV
Ga 3d
hv = 80 eV
Pd / GaAs (110)
0.05
0.2
0.5
0
1
2.5
5
10
24
50
0.1
N(E) (arbitrary units)
47.50
45.00
46.00
44.00
BINDING ENERGY (eV)

Figure 4

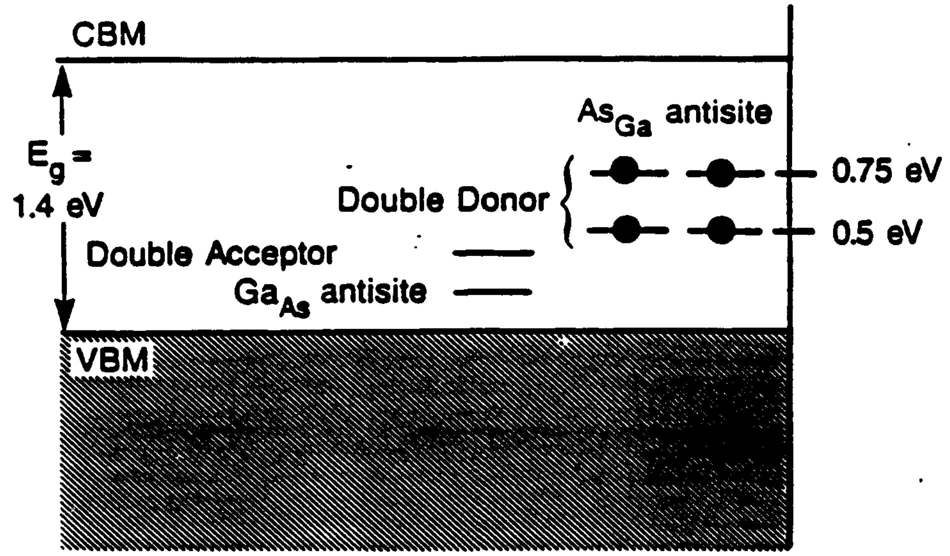

ADVANCED UNIFIED DEFECT MODEL

Figure 7

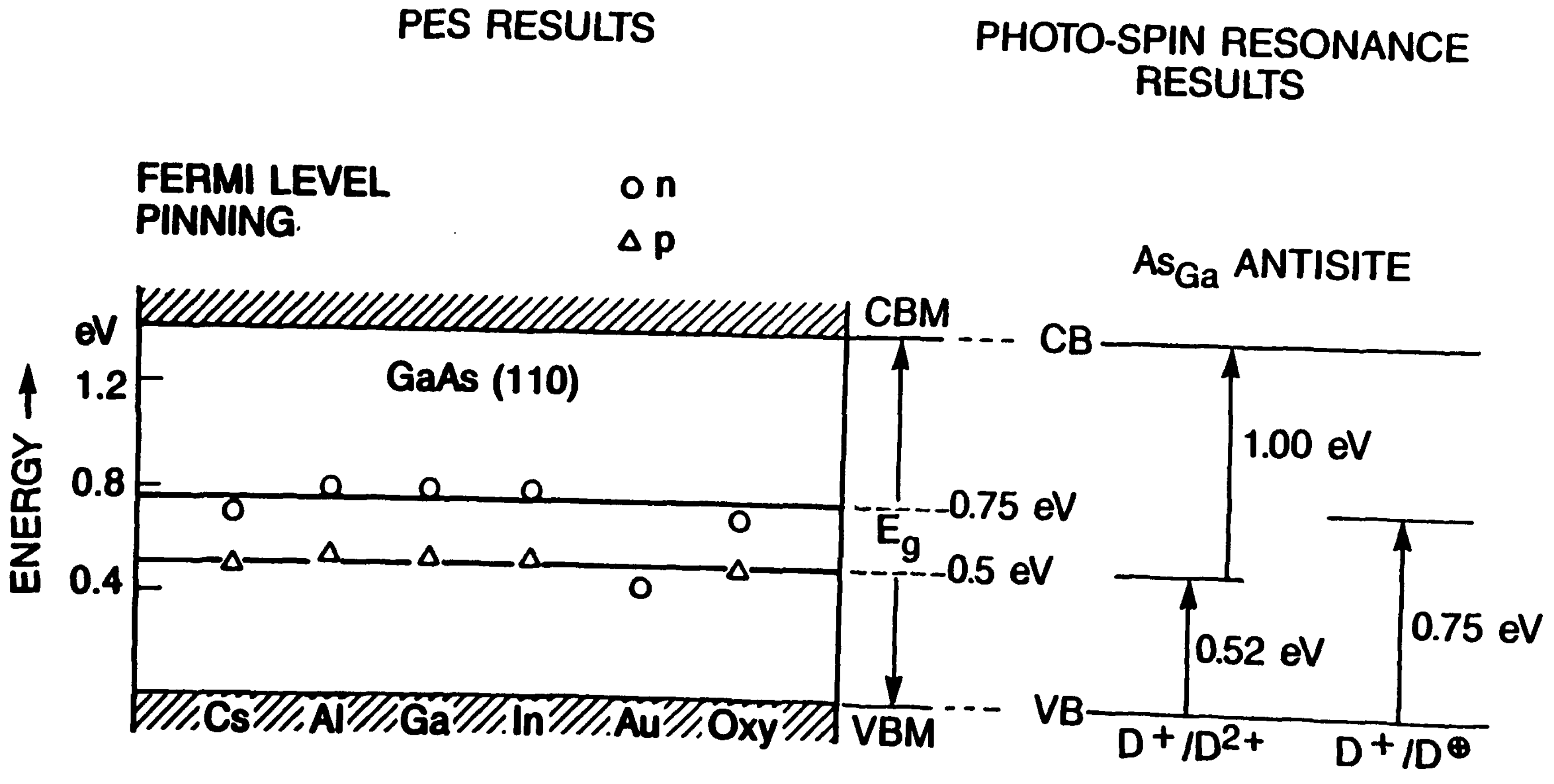

Spicer et al., 1979

Weber et al., 1982

Figure

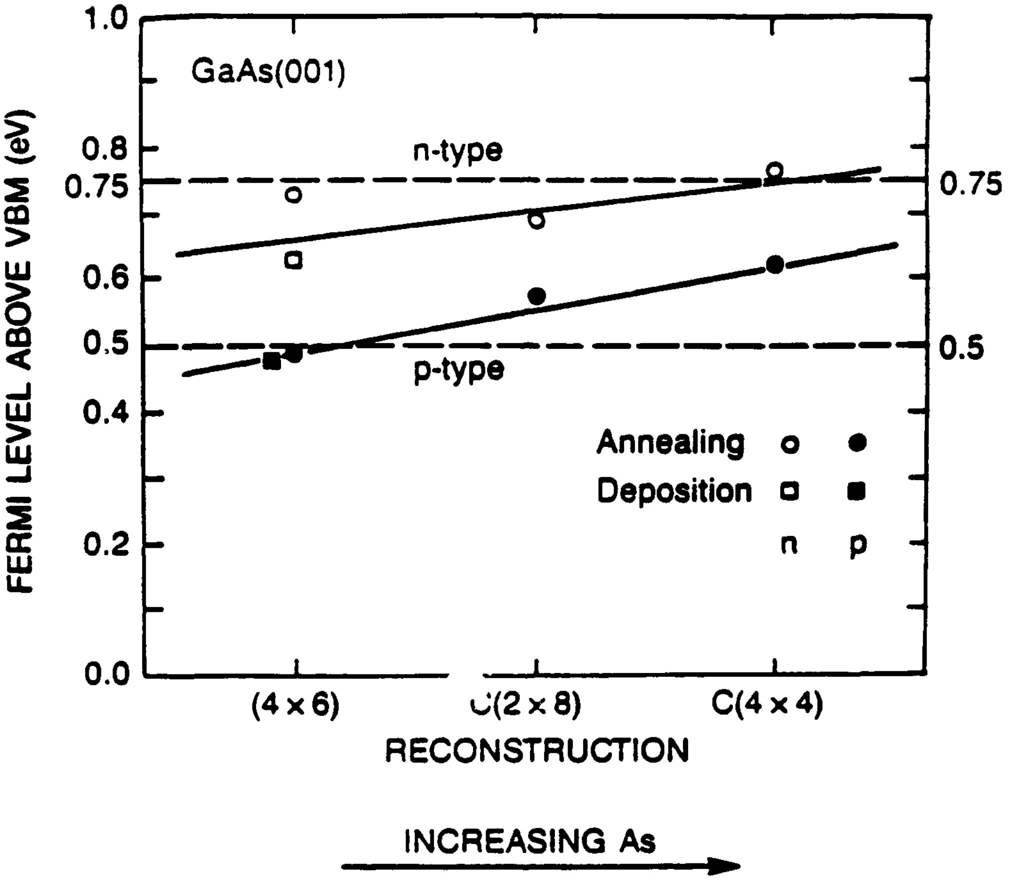

from: Svensson et al., *J. Vac. Sci. & Tech.* B2, 235 (1984)

Figure 9

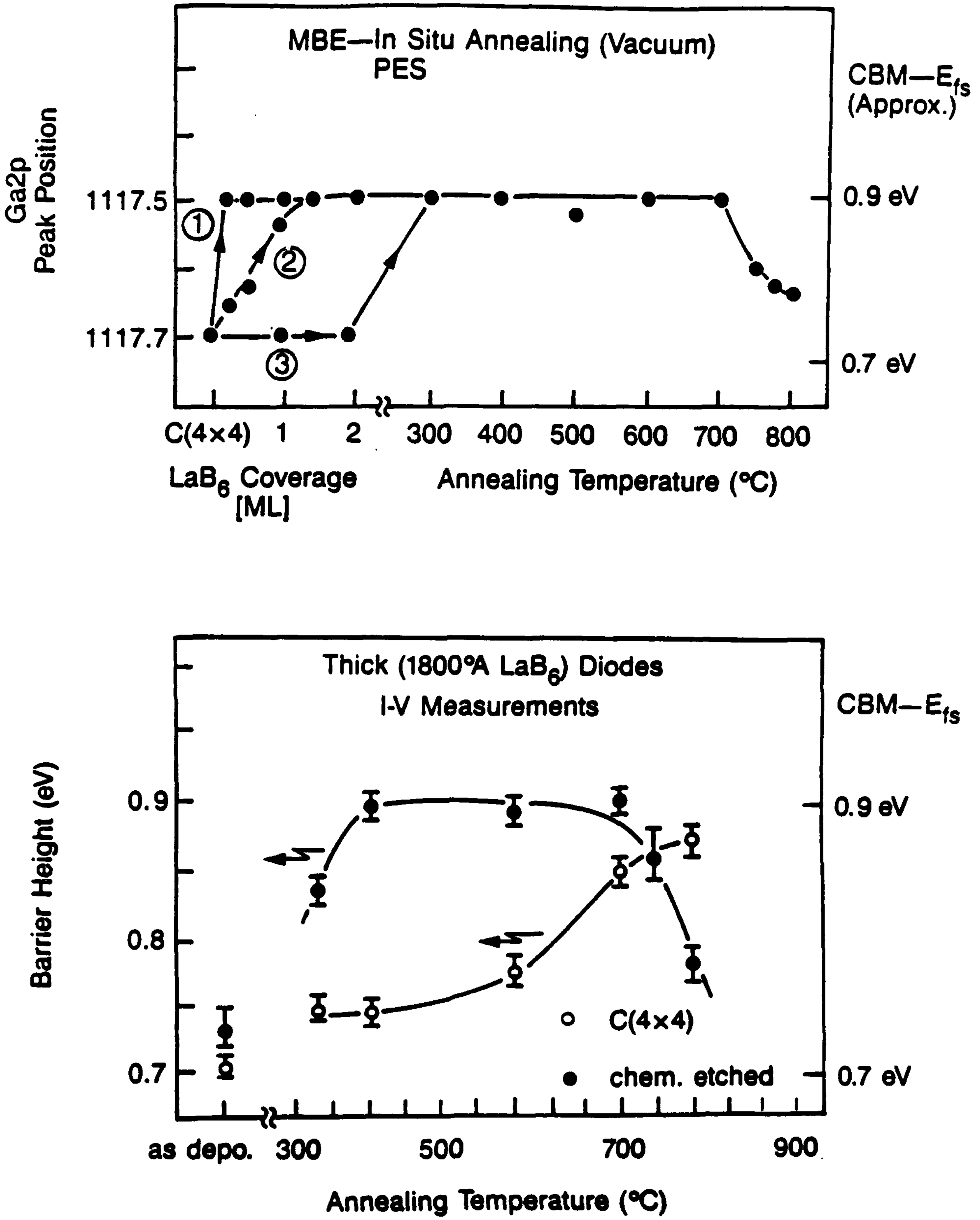

T. Yokatsuka, et al., Appl. Phys. Lett. *50*, 591 (1987)
Y. Uchida, et al., Appl. Phys. Lett. *50*, 670 (1987)

Figure 15

R. W. Grant and J. R. Waldrop: Variation of n-GaAs (100) interface Fermi level

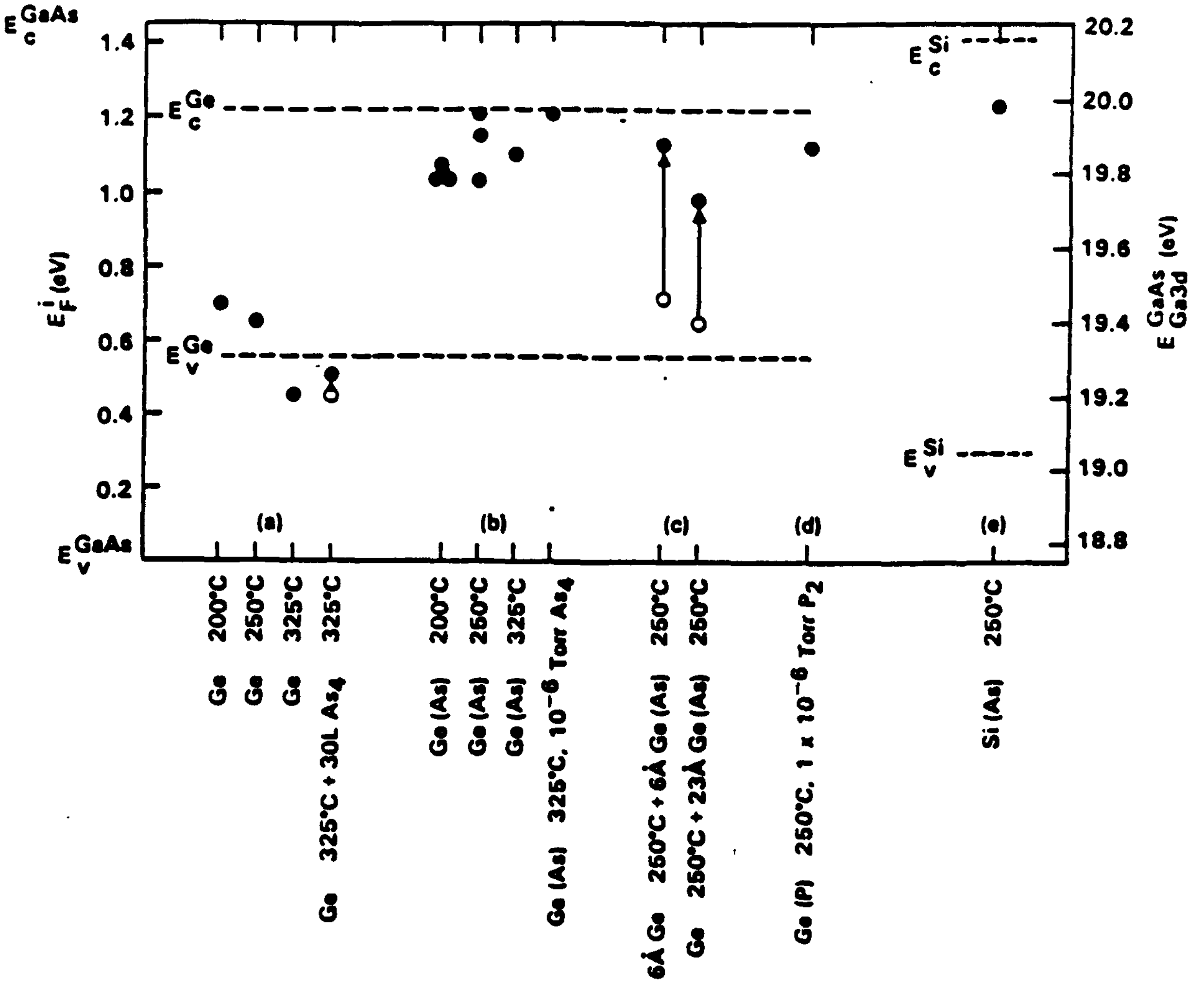

Figure 11

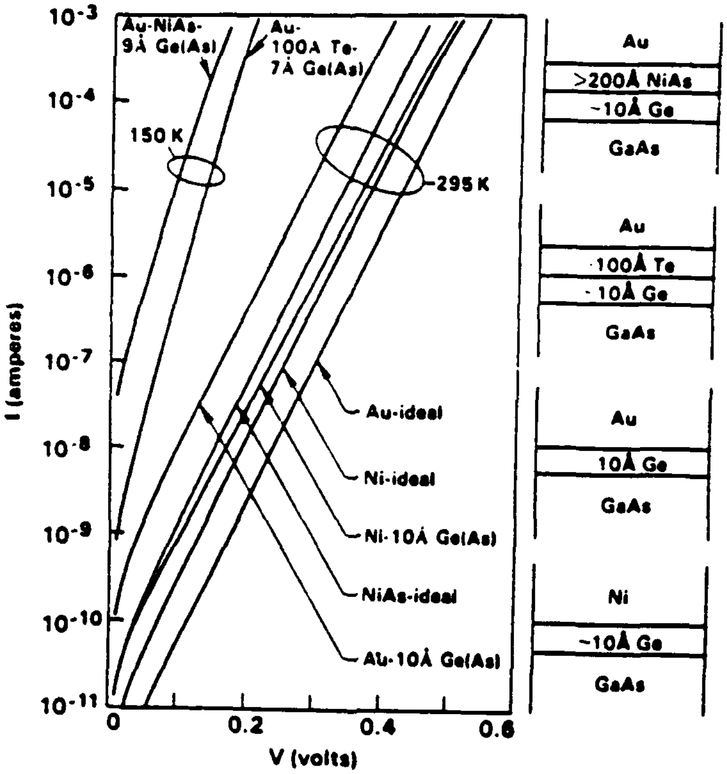

J. R. Waldrop and R.W. Grant
Appl. Phys. Lett. 50 (5) (1987)250.

Figure 12

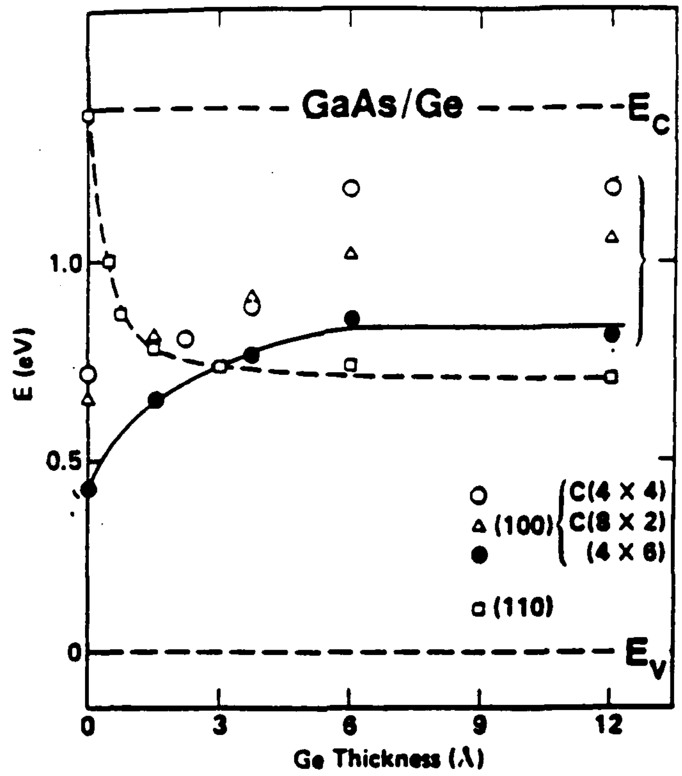
GaAs/Ge
E_C
E_V
E (eV)
1.0
0.5
0
0
3
6
9
12
Ge Thickness (Å)
○ (100) C(4 × 4)
△ (100) C(8 × 2)
● (100) (4 × 6)
□ (110)

Figure 13

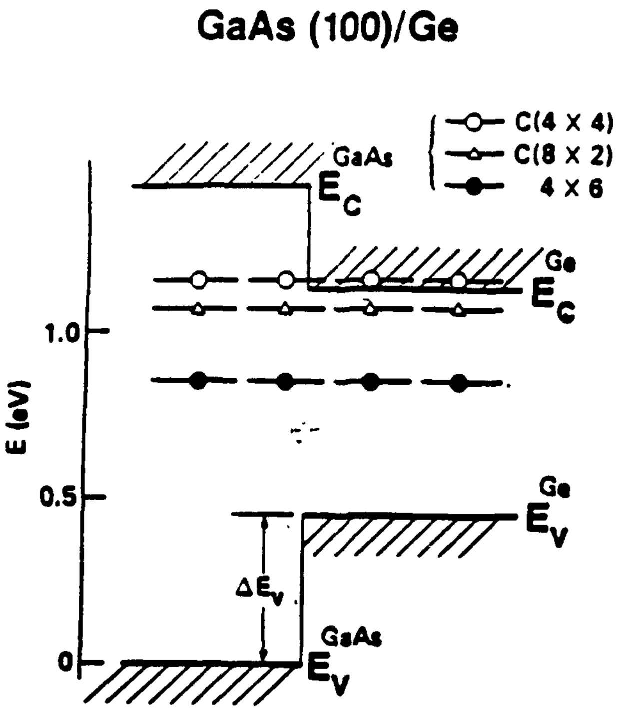
GaAs (100)/Ge
C(4 X 4)
C(8 X 2)
4 X 6
E (eV)
1.0
0.5
0
E_C^{GaAs}
E_C^{Ge}
E_V^{Ge}
E_V^{GaAs}
ΔE_V

Figure 14

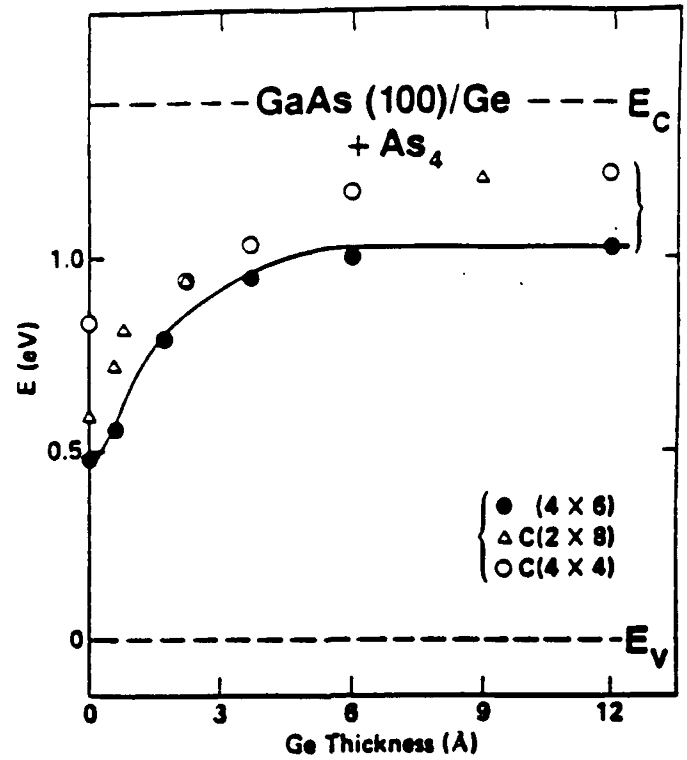
GaAs (100)/Ge
+ As$_4$
E_C
E_V
E (eV)
1.0
0.5
0
0
3
6
9
12
Ge Thickness (Å)
● (4 X 6)
△ C(2 X 8)
○ C(4 X 4)

Figure 15

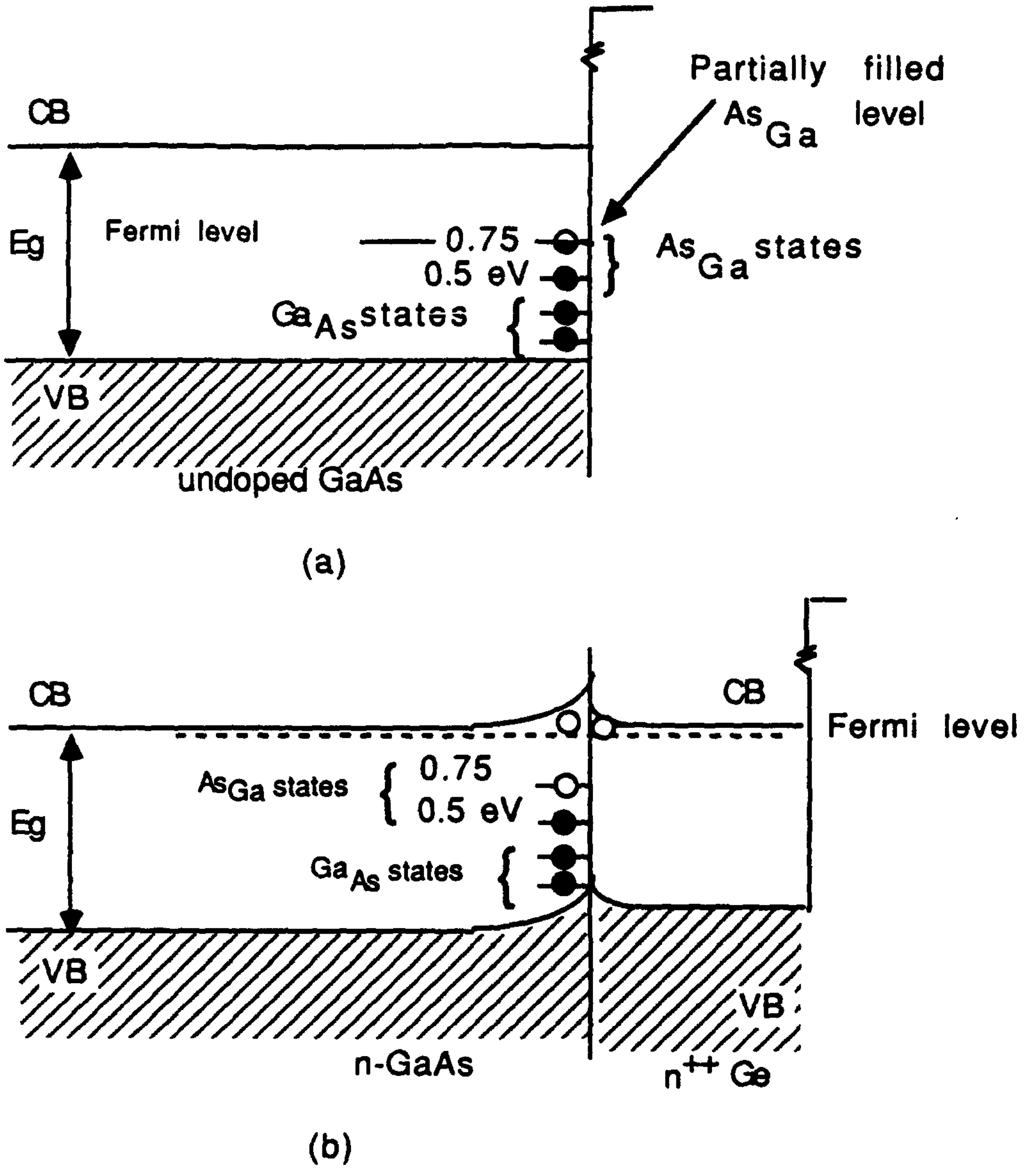
Partially filled
As_{Ga} level
CB
Eg
Fermi level
0.75
0.5 eV
As_{Ga} states
Ga_{As} states
VB
undoped GaAs
CB
Eg
As_{Ga} states
0.75
0.5 eV
Ga_{As} states
VB
n-GaAs
CB
Fermi level
VB
n^{++} Ge

(a)

(b)

Figure 16

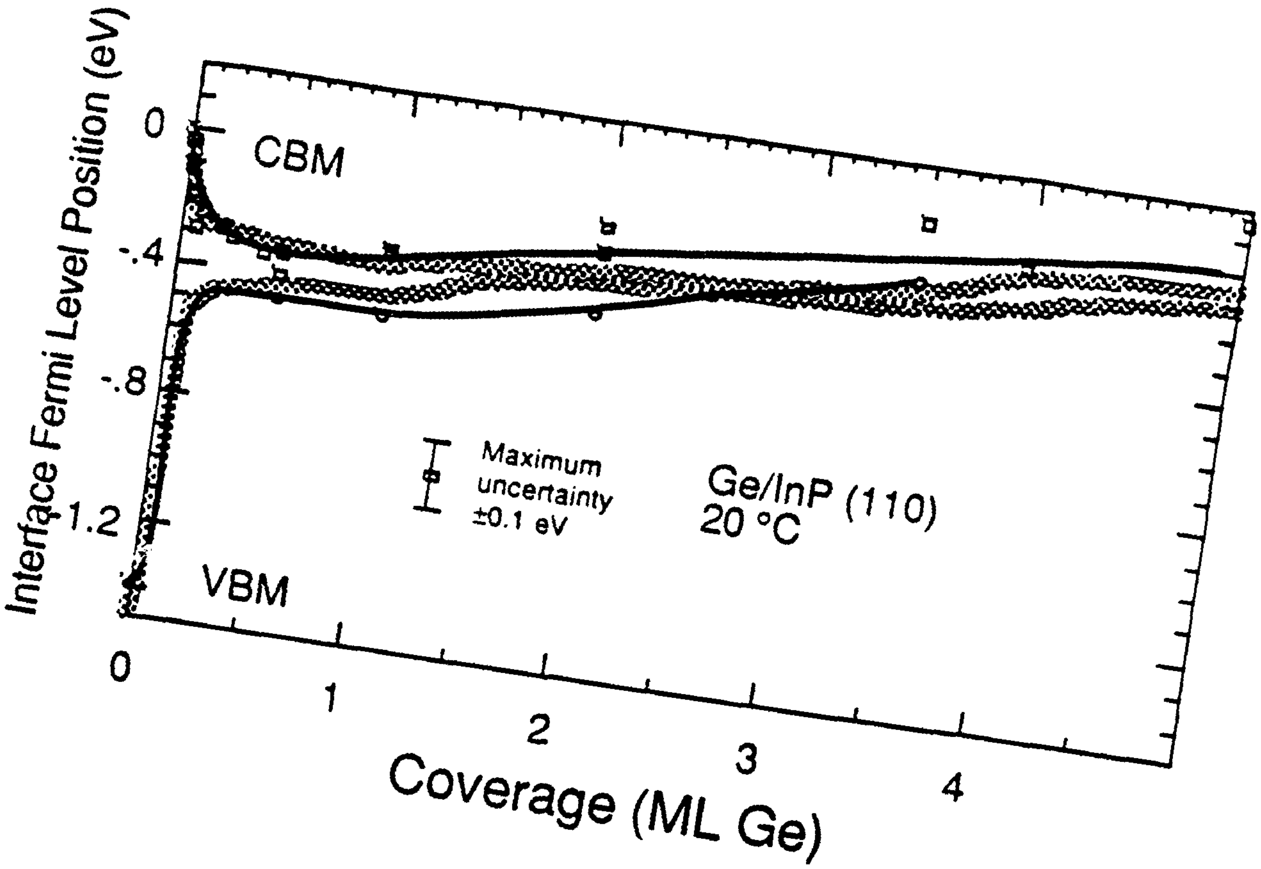
Interface Fermi Level Position (eV)
0
-.4
-.8
-1.2
CBM
VBM
Maximum
uncertainty
±0.1 eV
Ge/InP (110)
20 °C
0
1
2
3
4
Coverage (ML Ge)

Figure 17

Pd/Ge/GaAs Ohmic Contacts

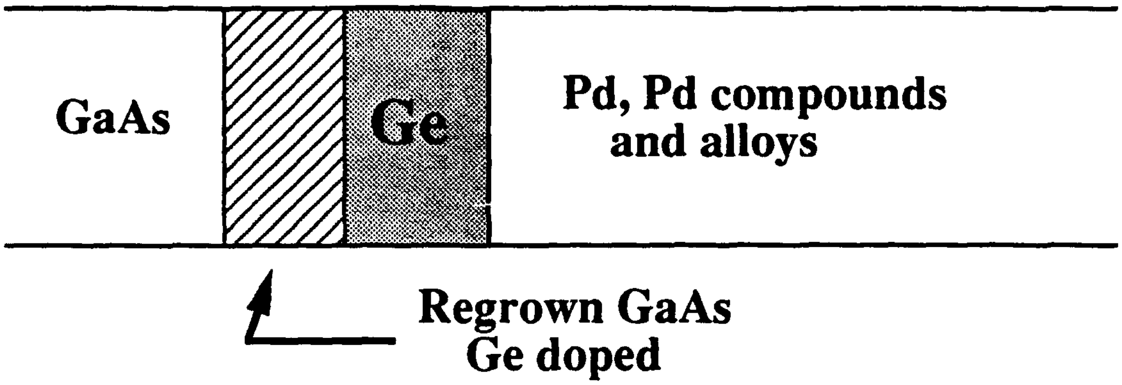

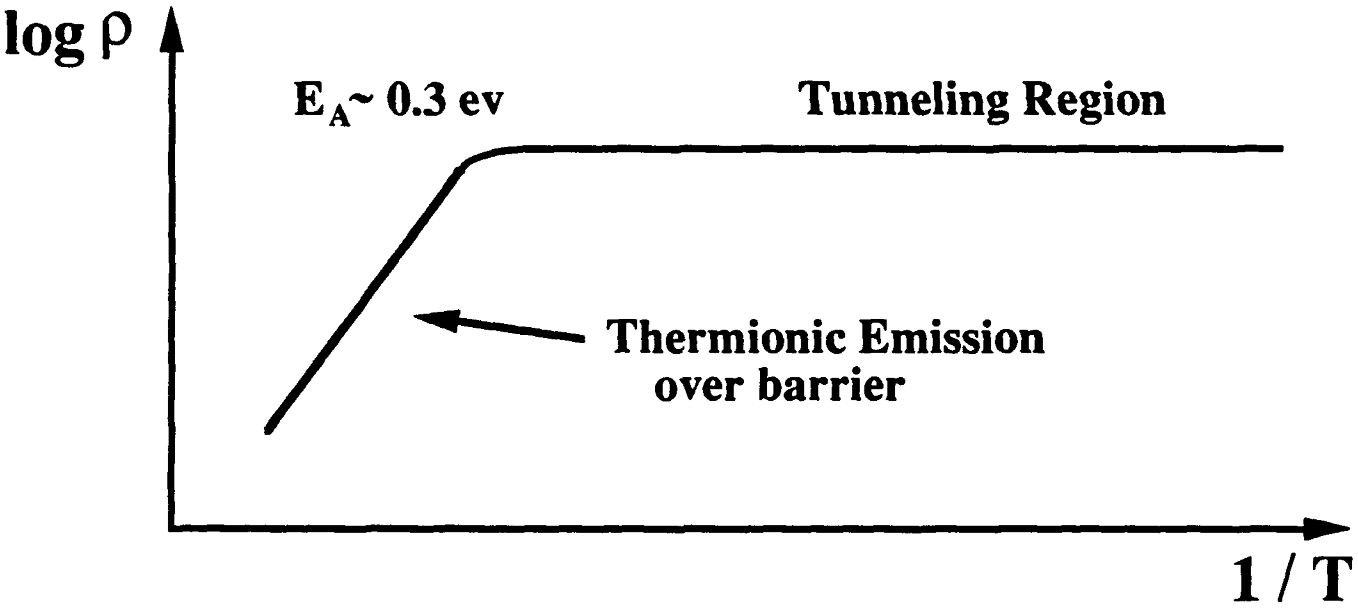

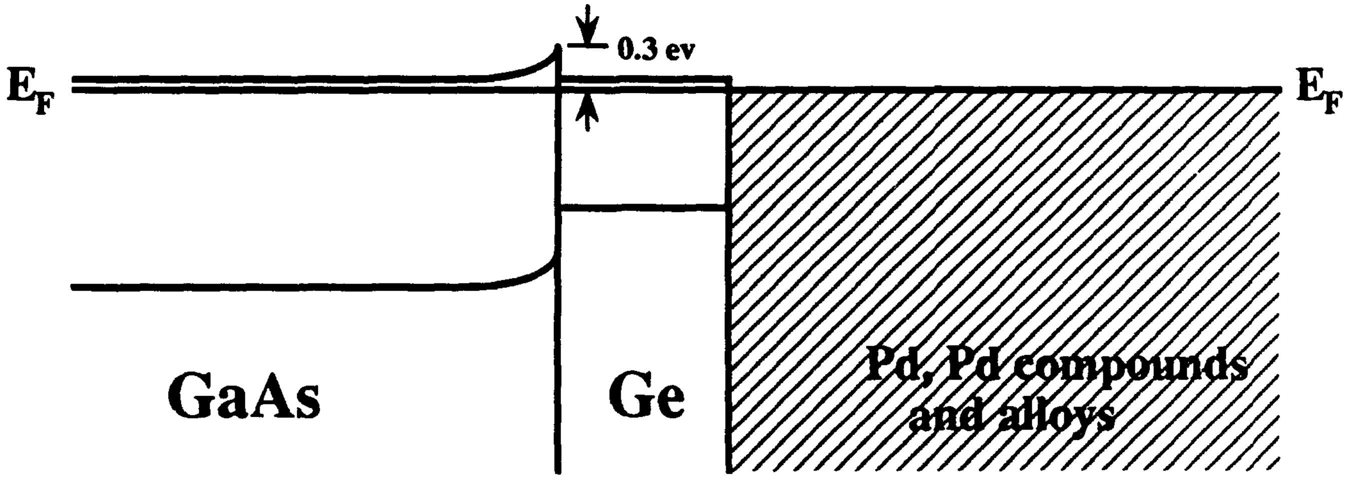

Figure 18

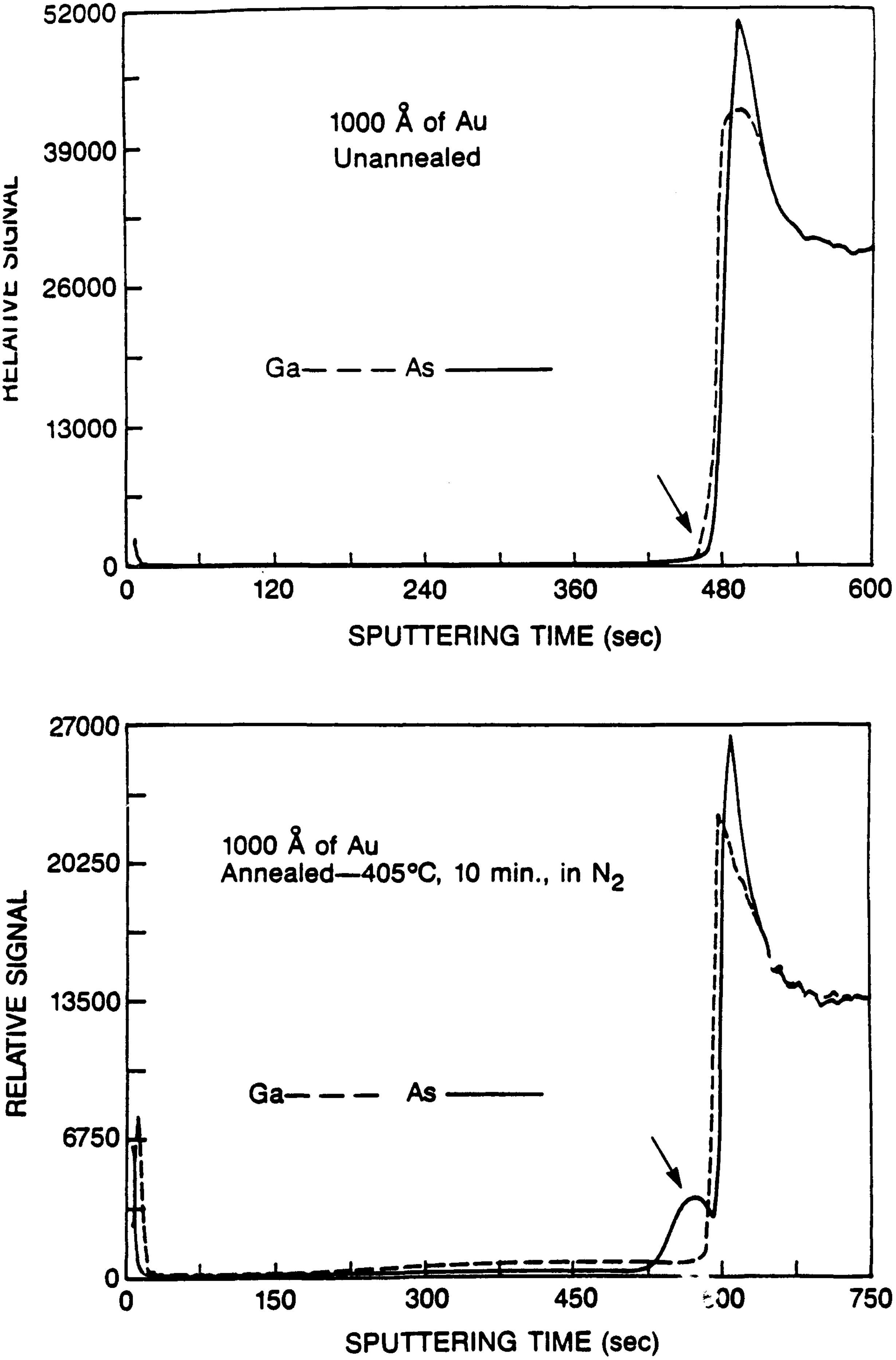

Pallix et al., MRS Bulletin 12, 52 (1987)

Figure 12

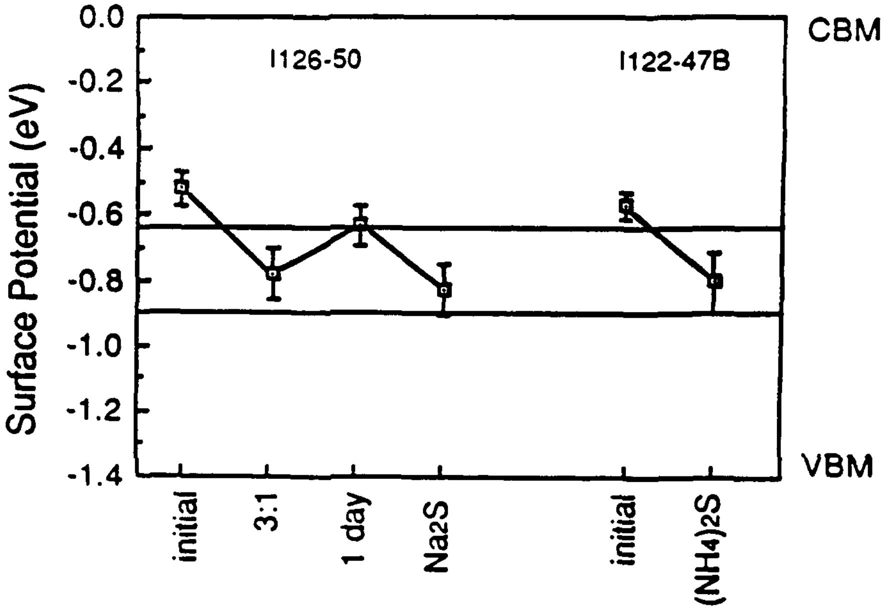

R. Besser et al.

Figure 20

Before Sulfur Treatment

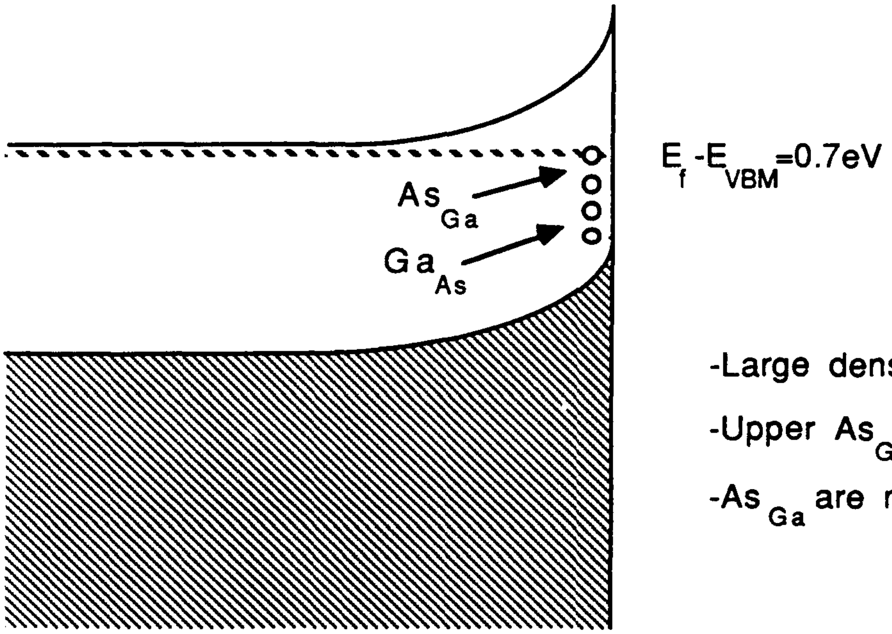

- Large density of As_{Ga} antisites
- Upper As_{Ga} level filled
- As_{Ga} are nuetral-good hole trap

After Sulfur treatment

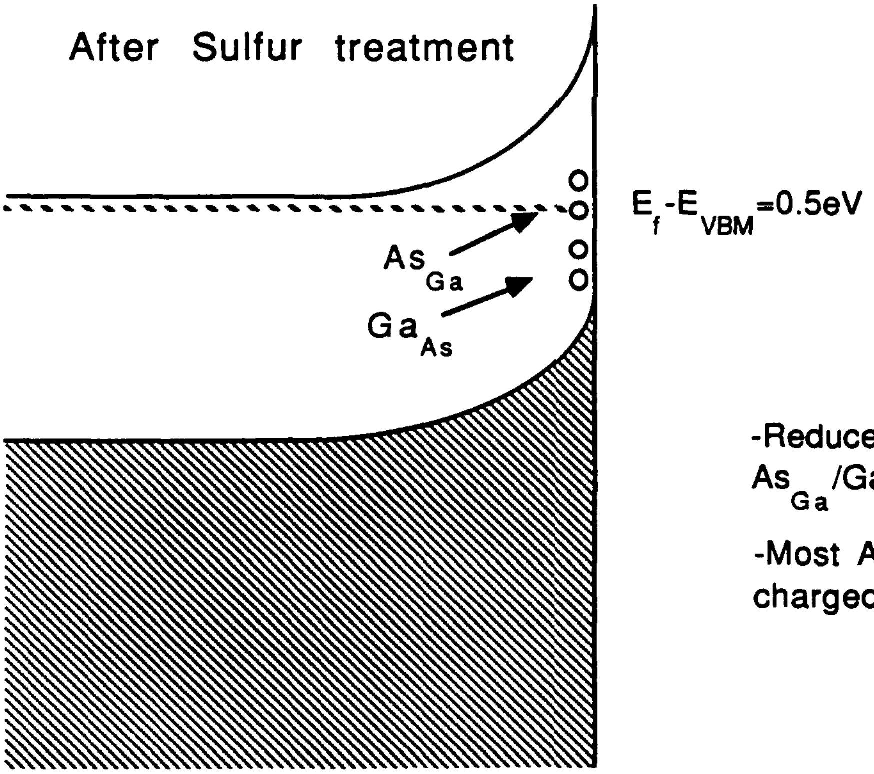

- Reduced As_{Ga} Density and As_{Ga}/Ga_{As} ratio
- Most As_{Ga} are positively charged-poor hole trapping.

Fig. 2

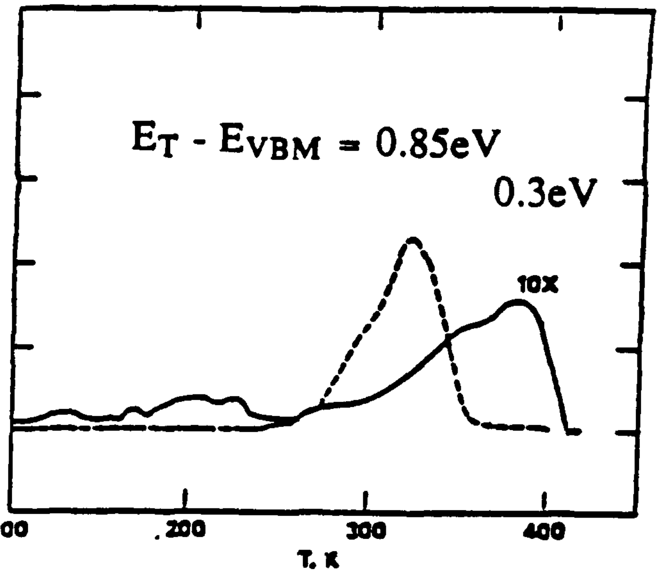

Figure ~~21~~ 22

III. Accomplishment Under This Contract - References are to number of paper published under this contract.

1. **Excess of As at Metal/GaAs Interfaces.** Using EDAX techniques it was established that Excess As is present at GaAs interfaces. This is important in determining that extrinsic (i.e. defect) mechanism are important in determining electrical properties (such as Schottky barrier heights) at metal/GaAs interfaces. [Ref. 4,5,13,14]

2. **Change in As Excess at Metal/GaAs Interface due to Thermal Annealing and Correlation with Changes in Barrier Height.** Using EDAX, it was established that the As excess at the interfaces is changed by annealing. If As excess increases, it was found that Schottky barrier height on n-GaAs decreased; whereas, if As excess decreased, the Schottky barrier height increased. [Ref. 1,4,5,13,14]

3. **Increase or Decrease in As Excess and Corresponding Change in Barrier Height Correlates with Production of Excess As or Ga by Metal/GaAs Chemical Reaction:** An important part of the PES work under DARPA and ONR support was establishing that chemical reactions take place between GaAs and metals. A key result under this contract was establishing that the excess As or Ga produced by such reactions, correlated with changes in Schottky barrier height. Thus, the interface chemistry could be correlated with changes in electrical properties of the interface. [Ref. 1,4,5,8,9,13,14]

4. **Development of the Advanced Unified Defect Model.** This model applies when native antisite defects dominate at the interface. Data obtained under this contract played a key role in the development of this model. As section II shows, it explains a wide range of metal/GaAs performance and gives a basis for optimizing GaAs Schottky barriers and ohmic contacts. It appears to apply in most (perhaps all) GaAs/metal contacts of practical interest. It gives a method for providing very stable, long lived GaAs/metal contacts. [Ref. 1,4,5,8]

5. **A Basis for Developing Schottky Barriers with very Stable Barrier Heights Over Their Lives:** Changes of Schottky barrier height with annealing agree well with aging results of FET's obtained by Varian (Ti Schottky gates). Thus it appears that results under this contract and the Advanced Defect Model can play a key role in developing stable Schottky barrier heights. Strong insights have also been obtained on the development of leakage currents during the life of a device. [Ref. 4,5,13,14]

6. **Oxide at Interface Can Enhance Change in Barrier Height Due to Stress by Electrical Current.** Studies of changes in barrier height due to Electrical aging of Schottky barriers show that, with some metals, the changes are strongly increased.

7. **A few layers of oxide at GaAs interface can massively effect the morphology of Au/GaAs interface.** For example, with a clean interface, an atomically smooth Au/GaAs interface is formed. With air exposed GaAs (producing a few monolayers of oxide), the interface is dominated by protrusion which extend a hundred Angstroms or more into the GaAs. Such protrusions can destroy device performance with closely spaced ohmic contacts (Ni/Au/Ge ohmic contacts or Au Schottky barriers. [Ref. 2,3,10]

8. **Adhesion of Metallization on GaAs:** Considerable understanding has been obtained of the factors leading to poor adhesion of metallization on GaAs. Poor

adhesion was found to occur when oxide was present on the GaAs and the metal applied did not react strongly with the oxide or the GaAs. [Ref. 12]

9. Basis for a More Scientific GaAs Metallization Technology: The work under this contract provides basic understanding which can provide a more scientific approach to GaAs metallization. This, in turn, can increase production yields and increase reliability of GaAs devices making GaAs more acceptable and economic. More work is needed to systematize and provide additional information if the full potential of this approach is to be realized. [Ref. 1-14]

Paper Published Under This Contract

1. Mechanism for annealing-induced changes in the electrical characteristics of Al/GaAs and Al/.InP Schottky contacts, N. Newman, W. E. Spicer, and E. R. Weber, *J. Vac. Sci. Tech.* **B 5** (1987) 1020.
2. Aging of Schottky diodes formed on air-exposed and atomically clean GaAs surfaces: An electrical study, A. Miret, N. Newman, E. R. Weber, Z. Liliental-Weber and J. Washburn, W. E. Spicer, *J. Appl. Phys.* **63** (1988) 2006-2010.
3. Schottky barrier instabilities due to contamination, N. Newman, Z. Liliental-Weber, E. R. Weber, J. Washburn, and W. E. Spicer, *Appl. Phys. Lett.* **53** (1988) 145-147.
4. The Advanced Unified Defect Model for Schottky Barrier Formation, W. E. Spicer, Z. Liliental-Weber, E. Weber, N. Newman, T. Kendelewicz, R. Cao, C. McCants, P. Mahowald, K. Miyano, and I. Lindau, *J. Vac. Sci. Technol. B* **6** (1988) 1245-1251.
5. The Influence of Current Stressing on the Structure of Ag Contacts to GaAs, Z. Liliental-Weber, A. Miret-Goutier, N. Newman, C. Jou, W. E. Spicer, J. Washburn, and E. R. Weber, *Mat. Res. Soc. Symp. Proc* **102** (1988) 241-244.
6. The Advanced Unified Defect Model and Its Applications, W. E. Spicer, T. Kendelewicz, N. Newman, R. Cao, C. McCants, K. Miyano, I. Lindau, Z. Liliental-Weber and E.R. Weber, *Applied Surface Science* **33/34** (1988) 1009-1029.
7. Schottky Barrier Instabilities Due to Contamination, N. Newman, Z. Liliental-Weber, E. R. Weber, J. Washburn and W. E. Spicer, *Appl. Phys. Let.t.* **53,** 145 (1988).
8. Disruption, Metallization, and Electrical Properties of Metal GaAs and InP Semiconductor Interfaces, W. E. Spicer, R. Cao, K. Miyano, C. McCants, T. T. Chiang, C. J. Spindt, N. Newman, T. Kendelewicz, I. Lindau, E. Weber and Z. Liliental-Weber, from Metallization and Metal-Semiconductor Interfaces, Ed. by Inder P. Batra, Plenum Publishing Corporation, p. 139-161, 1989
9. From Synchrotron Radiation to I-V Measurements of GaAs Schottky Barrier Formation, W. E. Spicer, R. Cao, K. Miyano, T. Kendelewicz, I. Lindau, E. Weber, Z. Liliental-Weber, and N. Newman, *Appl. Surf. Sci.* **41/42** (1989) 1-16.
10. Influence of Interfacial Contamination on the Structure and Barrier Height of Cr/GaAs Schottky Contacts, Z. Liliental-Weber, N. Newman, J. Washburn, E. R. Weber and W. E. Spicer, *Appl. Phys. Lett.* **54,** 356 (1989).

11. Mechanism for Nearly-ohmic Behavior in Annealed Au/n-GaAs Schottky Diodes, R. P. Leon, N. Newman, Z. Liliental-Weber, E. R. Weber, J. Washburn, and W. E. Spicer, *J. Appl. Phys.* **66**, 711 (1989).

12. W. E. Spicer, Adhesion of Metals to GaAs, Invited Paper, 1989 Spring Meeting of American Physical Society (Abstract published in Bulletin of American Physical Society, 1989)

13. "Pinning" and Fermi level movement at GaAs surfaces and interfaces, W. E. Spicer, N. Newman, C. J. Spindt, Z. Liliental-Weber, and E. R. Weber, J. Vac. Sci. Technol. A **8**, 2084-2089 (1990).

14. W. E. Spicer, Defects in Metal/III-V Heterostructures, book chapter to be published in Defects in III-V Compound Semiconductors, Ed. Eicke R. Weber, Academic Press, Inc.